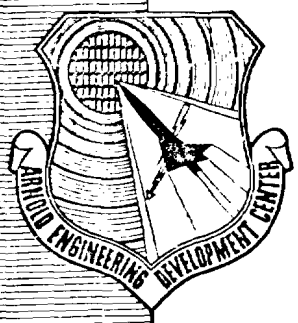

COMMENTS ON THE USE OF COMBUSTION GASES AS AN AERODYNAMIC TEST MEDIUM

By

M. H. Nesbitt and L. R. Carpenter
Propulsion Wind Tunnel Facility
ARO, Inc.

TECHNICAL DOCUMENTARY REPORT NO. AEDC-TDR-62-38

May 1962

AFSC Program Area 806A, Project 8951, Task 89106

(Prepared under Contract No. AF 40(600)-800 S/A 24(61-73) by ARO, Inc., contract operator of AEDC, Arnold Air Force Station, Tennessee.)

ARNOLD ENGINEERING DEVELOPMENT CENTER

AIR FORCE SYSTEMS COMMAND

UNITED STATES AIR FORCE

COMMENTS ON THE USE OF COMBUSTION GASES AS AN AERODYNAMIC TEST MEDIUM

By

M. H. Nesbitt and L. R. Carpenter

Propulsion Wind Tunnel Facility

ARO, Inc.,
a subsidiary of Sverdrup and Parcel, Inc.

May 1962

ARO Project No. 206099

ABSTRACT

Theoretical and experimental studies of pressure and heat transfer distributions for simple bodies at a Mach number of about 6.5 and a stagnation temperature of about 3000°R have been accomplished using both air and combustion gas as the testing media.

The purpose of this report is to (1) summarize the results of these studies, (2) compare results obtained in air and combustion gas by theory and by experiment, (3) point out the apparent differences encountered if combustion gases are used as a test medium instead of air, and (4) describe the testing difficulties that would be encountered with the use of combustion gases.

The experimental differences between test media indicate that the use of combustion gases in the regime investigated does not appear promising. Gas-liquid phase changes caused test complication, and the attendant test results were difficult to interpret or adjust to actual flight conditions.

CONTENTS

		Page
	ABSTRACT	iii
	NOMENCLATURE	vii
1.0	INTRODUCTION	1
2.0	SUMMARY OF PREVIOUS WORK	
	2.1 Analytical Part (Ref. 1)	1
	2.2 Experimental Part (Ref. 2)	3
3.0	DISCUSSION	
	3.1 Water Vapor Condensation	4
	3.2 Comparison of Various Test Media	5
	3.3 Effects of Non-Equilibrium Flow Conditions	11
	3.4 Testing and Operating Difficulties	14
4.0	CONCLUDING REMARKS	14
	REFERENCES	16
	APPENDIX	18

TABLES

1. Percentage Difference in the Parameter p_ℓ/p_∞ for the 10-deg Half-Angle Blunted Cone, α = 0 deg 21
2. Percentage Difference in the Parameter p_ℓ/p_∞ for the Flared Hemispherical Cylinder, α = 0 deg 22
3. Percentage Difference in the Parameter p_ℓ/p_∞ for the 6-deg Half-Angle Double Wedge 23
4. Percentage Difference in Heat Transfer Rates $(\dot{q}/\dot{q}_o)$ for the Flared Hemispherical Cylinder, α = 0 deg 24
5. Percentage Difference in the Heat Transfer Coefficient, h, for the 6-deg Half-Angle Double Wedge 25
6. Vibrational Relaxation Characteristics for Various Gases at Low Temperatures and One Atmosphere 26

ILLUSTRATIONS

Figure

1. Geometric Characteristics of Bodies 27
2. Schematic of the Hypersonic Blowdown Wind Tunnel, Test Section 12 by 12 in., Rosemount Aeronautical Laboratory, University of Minnesota 28

Figure		Page
3.	Partial Pressure of Water Vapor in an Isentropic Nozzle	29
4.	Wind Tunnel Water Vapor Supersaturation Characteristics as Given by Ref. 4	30
5.	Tunnel Sidewall Centerline Static Pressure Distributions	31
6.	Pressure Distribution on a 10-deg Half-Angle Blunted Cone, α = 0 deg	
	a. p_ℓ/p_∞	32
	b. p_ℓ/p_t'	33
7.	Pressure Distribution on the Flared Hemispherical Cylinder, α = 0 deg	
	a. p_ℓ/p_∞	34
	b. p_ℓ/p_t'	35
8.	Pressure Distribution, p_ℓ/p_∞, on a Blunted 6-deg Half-Angle Double Wedge	
	a. α = 0 deg	36
	b. α = 5 deg	37
	c. α = 10 deg	38
	d. α = 15 deg	39
9.	Schlieren Photograph of Blunted 6-deg Half-Angle Double Wedge, Dry Air, p_t = 130 psia, T_t = 2600°R, α = 10 deg	40
10.	Comparison of Wave Patterns Between Air and Combustion Gas on a Blunted 6-deg Half-Angle Double Wedge, α = 10 deg	41
11.	Lift as a Function of Angle of Attack for the Blunted 6-deg Half-Angle Double Wedge	42
12.	Heat Transfer Rate Distribution on the Flared Hemispherical Cylinder, α = 0 deg	43
13.	Heat Transfer Coefficient Distribution on Blunted 6-deg Half-Angle Double Wedge	
	a. α = 0 deg	44
	b. α = 5 deg	45
	c. α = 10 deg	46
	d. α = 15 deg	47
14.	Equilibrium Composition of Air and Combustion Gases	
	a. Combustion Gas, C_2H_4 and Air at f/a = 0.06, $\rho/\rho_o = 10^{-2}$	48
	b. Air, $\rho/\rho_o = 10^{-2}$	49

NOMENCLATURE

A	Reference area, ft^2
C_N	Normal force coefficient
c	Chord length of double wedge, 10.96 in.
D	Cone base diameter, 5.5 in.
f/a	Fuel air ratio
g	Gravitational constant, ft/sec^2
h	Convective heat transfer coefficient, Btu/ft^2-sec-°R
M	Mach number
p	Pressure, psia
$\dot{q}$	Local heating rate, Btu/ft^2-sec
$\dot{q}_o$	Stagnation point heating rate, Btu/ft^2-sec
R	Gas constant, ft-lbf/lbm-°R
R	Body nose radius, in.
S	Distance along surface, in.
T	Temperature, °R
ΔT	Degree of subcooling, °R
u	Velocity, ft/sec
x	Axial distance, in.
Y	Ordinate of tunnel nozzle, in.
Z	Altitude, ft
α	Angle of attack, deg
γ	Specific heat ratio
θ	Angle from body centerline to locus of point on hemisphere - Configuration 2, deg
λ	Shock stand-off distance, in.
μ	Viscosity, lbm/ft-sec
ρ	Gas density, lbm/ft^3
Ω	Absolute humidity, lbm water vapor/lbm dry gas

SUBSCRIPTS

cg	Combustion gas
L	Lower surface
ℓ	Local model conditions
o	Standard pressure and temperature conditions
t	Stagnation
U	Upper surface
v	Vapor
δ	Edge of boundary layer
∞	Free stream
2	Conditions downstream of normal shock

SUPERSCRIPTS

'	At body stagnation point
*	Eckert's reference conditions

1.0 INTRODUCTION

Various gas dynamic test facilities have employed products of combustion as test media because of the relative ease with which large mass flows of hot gases may be obtained. Hydrocarbon fuel and air is the fuel-oxidizer combination most frequently used. Since the combustion gases resulting with this combination have a large water vapor content and since their thermal, transport, and chemical properties differ from those of air, difficulties arise in interpreting results to the flow of air. Moreover, comparative test results measured in both air and hydrocarbon combustion gas test media are generally not available. Consequently, the actual differences which would result by testing in a combustion gas are not known. For these reasons, the Arnold Engineering Development Center (AEDC), Air Force Systems Command (AFSC), initiated a joint effort between ARO, Inc. and the Rosemount Aeronautical Laboratory to determine these differences both analytically and experimentally.

The analytical part (Ref. 1) of this work made predictions of pressure and heating rate distributions for simple aerodynamic shapes assuming both air and combustion gas test media at a Mach number of about 6.5 and at a stagnation temperature of 3000°R. The experimental part (Ref. 2) was carried out at the Rosemount Aeronautical Laboratory and was designed to provide experimental data for comparison with theory and to determine the effects of water vapor condensation when combustion gas test media are used.

A brief resumé of each of these parts is given here. However, the purpose of this report is to (1) combine and summarize the important findings of both of these studies and (2) point out problems and areas of interest not previously covered in Refs. 1 and 2.

2.0 SUMMARY OF PREVIOUS WORK

2.1 ANALYTICAL PART (Ref. 1)

Thermodynamic properties important to gas dynamics of a typical hydrocarbon combustion gas (C_2H_4 and 200-percent theoretical air) were theoretically determined. Analytical predictions of the pressure and heat

Manuscript released for printing May 1962.

transfer rate distributions over three simple aerodynamic shapes (a blunted cone, a hemisphere-cylinder-flare body of revolution, also called the blunt body, and a two-dimensional double wedge) (see Fig. 1) were then made assuming both air and combustion gas test media. These calculations were based on the following nominal flow conditions:

Air	Combustion Gas (C_2H_4 and 200-Percent Theoretical Air)
M_∞ = 6.70	M_∞ = 6.51
p_t = 130 psia	p_t = 123 to 128 psia
T_t = 3000°R	T_t = 3000°R

The flow is considered inviscid for all calculations, and for simplicity, any effects of water condensation were neglected even though condensation was expected to occur during the experimental phase. This study only attempted to define differences that would be obtained in a combustion gas test medium because of its different thermal and transport properties. Both test media were assumed to always be in equilibrium, and vibrational real gas effects were taken into account.

The pressure distribution was obtained for the blunted cone, Configuration 1, using conical flow parameters for various specific heat ratios from Ref. 3. Newtonian, Prandtl-Meyer, and blast wave theories were used to estimate the pressure distribution of the blunt re-entry body of revolution, Configuration 2, whereas for heat transfer rates the theories of Fay and Riddell and of Kemp, Rose, and Detra were employed. For the two-dimensional double wedge, Configuration 3, the shock-expansion method and Eckert's reference enthalpy method were used to determine the pressure distribution and heat transfer distribution, respectively.

As a result of these analytical computations it was concluded that, for a wind tunnel with a fixed geometry nozzle, small reductions in the stagnation pressure and temperature for combustion gas testing could result in rather closely matching air results for the surface pressure and heating rates over the forward portions of the bodies considered. However, significant percentage differences would still exist over the rear portions. The magnitude of these differences varied from body to body, but somewhat lower surface pressures (approximately 20 percent) and higher heating rates (up to 10 percent) were indicated for a combustion gas test medium. All of these differences would be caused by the different gas properties of air and combustion gases. They do not reflect any effects of gas-liquid phase changes in the combustion gas test medium.

2.2 EXPERIMENTAL PART (Ref. 2)

Pressure and heat transfer data were obtained experimentally in the 12 by 12-in. hypersonic tunnel at the Rosemount Aeronautical Laboratory (RAL) for the same bodies and test media assumed in the theoretical part. The test facility (Fig. 2) consists of two independent high-pressure storage systems valved through an aluminum oxide pebble-bed, gas-fired regenerative heater, fixed two-dimensional $M_\infty = 7$ (with dry air) nozzle blocks, motor-driven variable diffuser, and a vacuum storage.

To eliminate the hazards of burning, the combustion gas test medium was obtained by placing the components of the combustion gas mixture (assuming 100-percent combustion efficiency), less water vapor, in one of the high pressure storage tanks. These gases were heated to the simulated combustion temperature, and water was added and vaporized in the pebble-bed heater.

During the experimental tests it was found that water condensation in the wind tunnel nozzle significantly affected the test section flow conditions and the resulting test data. Therefore, tests of air mixed with the same amount of water vapor used during the combustion gas tests were also conducted. Also, some data were obtained with combustion products containing no water vapor.

Nominal flow conditions in each test medium as given in Ref. 2, Table 4, are summarized below:

Symbols	Air	Air	Combustion Products	Combustion Products	Combustion Products
	$\Omega = 0$	$\Omega = 0.042$	$\Omega = 0$	$\Omega = 0.021$	$\Omega = 0.042$
p_∞/p_t'	1.759×10^{-2}	2.101×10^{-2}	1.844×10^{-2}	1.953×10^{-2}	2.054×10^{-2}
p_∞/p_t	2.966×10^{-4}	3.538×10^{-4}	3.085×10^{-4}	3.267×10^{-4}	3.437×10^{-4}
p_t	130 psia	130 psia	130 psia	130 psia	130 psia
T_t	2520°R	2612°R	2526°R	2570°R	2612°R
γ_∞	1.401	1.395	1.399	1.396	1.393
M_∞	6.594	6.039	6.442	6.262	6.111

A summary of the various configurations and test media included in the Ref. 2 investigation is given in the Appendix. Only selected pressure and heat transfer test results from the experimental phase are discussed here.

3.0 DISCUSSION

3.1 WATER VAPOR CONDENSATION

The experimental tests pointed out quite vividly the complications which would be introduced by a combustion gas test medium because of phase changes of the water formed during combustion. Condensation characteristics of the combustion gas test medium are shown in Fig. 3. Prior to the initiation of this phase, RAL personnel felt that on the basis of their previous experience with low humidity air, condensation would not occur until the expansion reached about the 90-deg supersaturation line shown in the figure (M_∞ = 7.0). Recent experimental work by Stepchkov in Russia (Ref. 4), however, indicates that the degree of supersaturation possible in wind tunnels decreases with increase of the water vapor content or specific humidity of the test medium. Stepchkov's work which was also conducted in a 12 by 12-in. tunnel has been extrapolated (Fig. 4) and illustrates that little supersaturation would occur with the water content of the combustion gases (Ω = 0.042) employed in this study. Nozzle wall static pressure distributions given in Ref. 2 (Fig. 5) indicate that the water condensed prior to the 8-in. station or at a Mach number less than 6.3 (in dry air). Also, the Fig. 3 analysis suggests that the water condensed at $M_\infty > 5.8$. Thus, it appears clear that condensation must have occurred near the vapor saturation line as indicated by Stepchkov's work, and one may not depend upon a significant degree of supersaturation with a combustion gas test medium.

As a result of water condensation within the tunnel nozzle, the determination of actual test section flow conditions became more complicated. Hermann et al (see Ref. 2, Appendix A) have concluded that the conventional adiabatic Rayleigh equation for p_∞/p_t' can be used to determine the test section Mach number in a condensing flow because it only involves measurements made downstream of where condensation occurred, while the usual ratios p_∞/p_t and p_t'/p_t would provide meaningless results. The effect of condensation is to increase the test section static pressure level and reduce the Mach number (see Fig. 5). Combustion gas Mach numbers of about 6.1 (compared to 6.6 for dry air) were indicated both by the Rayleigh equation and by the cone pressure distribution which incorporates a correction for the boundary-layer growth. A reduction of Mach number

in itself may not be a serious handicap in the hypersonic range where the Mach number independence principle holds and hence where aerodynamic phenomena vary only slightly with changes in M_∞. However, as shown in the next section, the interpretation of test data in such flows is extremely difficult or impossible. It is not clear just what thermodynamic properties should be associated with a test medium with a liquid component, or what influence the liquid particles exert upon the test bodies, or lastly, what phase equilibrium conditions exist following the shock fronts.

As shown in Fig. 3, condensation may be somewhat delayed by testing at lower pressures. Also, at first glance it might be thought that condensation could be greatly retarded or completely eliminated by employing a much higher temperature combustion gas (for example, $T_t \approx 4000°R$). This, however, as a general rule will not be the case. To achieve a higher temperature combustion gas, it is necessary to use much larger fuel-air ratios, which in turn results in a larger water vapor component. A larger water content causes condensation to occur sooner and counterbalances much of the effect of an increase in temperature. As a matter of interest, a hydrocarbon combustion gas with $T_t = 4000°R$ and $p_t = 2000$ psia would require a near stoichiometric fuel-air ratio and consequently begins to condense at a Mach number near 6.7, which is not greatly different from the conditions of the experimental tests. Moreover, if the tunnel nozzle expansion was completed somewhere short of the condensation point, water condensation might then occur as the fluid expands locally around the test body, resulting in local condensation shocks. In this case, test data would be even more difficult to interpret than if the condensation occurred entirely during the nozzle expansion.

3.2 COMPARISON OF VARIOUS TEST MEDIA

Because of the occurrence of water condensation during the experimental tests, a direct comparison of the Ref. 2 test results with the theoretical predictions of Ref. 1 would have little significance. Since techniques to examine the characteristics of two-phase flows are not well established, no further attempt has been made to refine the theoretical predictions. It is instructive, however, to examine the differences indicated between the various test media both by experiment and theory. Such comparisons indicate the effects of condensation on test data (from experimental tests) and effects due to the different gas properties of air and combustion gases (from theoretical analysis). By noting variation in measured differences between test media and by observing phenomena not predicted by the theory, conclusions may be drawn about the reliability of

data obtained when combustion products are used as the aerodynamic test medium. A comparison between the present experimental and analytical results point out some of the difficulties encountered in attempting to incrementally correct combustion gas results to the air case.

3.2.1 Pressure Distribution

Pressure distributions obtained for Configuration 1 are shown in Fig. 6. The irregular distribution along a conical surface is thought to be a true effect induced by the tip blunting. Lewis at AEDC (Ref. 5) has measured such a distribution, and Cheng, et al (Ref. 6) has theoretically predicted this phenomena. It might also be noted that base pressures were about 0.8 of the pressure on the short afterbody cylinder for both test media, which seems reasonable for this type configuration.

The level between experiment and theory differs even for an air test medium. Study of the Ref. 2 data indicates that this difference is associated with the interpretation of the experimental free-stream conditions. Reference 2 presents pressure distribution data (as shown in Fig. 6a) divided by a static pressure which was obtained from a test section calibration rake (see Section 2.2 of Ref. 2). If, however, the Fig. 6a air data are adjusted to ratios of the local cone surface pressure to the wall static pressure measured when the cone was in the tunnel, these pressure ratios fall quite near the theoretical estimate, and the conical pressure distribution represents a free-stream Mach number of about 6.6, which is consistent with the previous estimates. The difference between free-stream static pressures measured in these two ways is not fully understood, but it may be due to lateral or longitudinal pressure gradients. A similar shift will result if this procedure is applied to the combustion gas data.

Since there is no assurance that the wall static data better estimates the actual flow conditions in all cases, and condensation changes the experimental level for combustion gas in any case, the Ref. 2 values of p_ℓ/p_∞ have been retained in the analysis.* The uncertainty of the free-stream conditions should have only a small effect on the incremental difference between test media.

The surface pressures measured for the cone in an air test medium were on the average about 15 percent higher than those measured in

*Pressure coefficient data have not been considered in this report since the influence of nominal flow conditions even further complicates their analysis.

combustion gases (see Fig. 6a and Table 1). This difference is due to the combined effect of different thermal properties of the two media and condensation of the H_2O in the combustion gases. Simple conical-flow calculations assuming perfect gases indicate that an 8 to 10 percent difference would be expected because of the difference in gas properties between the test media. Consequently, condensation is believed to be responsible for the remaining difference or about 5 to 7 percent shift. The reduction of the test section Mach number for the combustion gas test medium due to condensation (shown in the table on page 3) also corresponds to a 5 to 7 percent lower conical pressure. Thus, the effect of condensation on the pressure distribution appears to be only associated with changes of the free-stream conditions. Air containing the same amount of water as the combustion gases produced pressures about 20 percent lower than those for dry air, which was a somewhat larger reduction than measured with combustion gases.

Pressure distributions obtained for Configuration 2 for dry air and combustion gas test media are given in Fig. 7a. The distributions produced by both test media are quite similar to those obtained by other investigators for hemisphere-cylinder bodies. The combustion gas test medium with water condensation in the tunnel nozzle produced about 15 to 20 percent lower pressures along the body than did air (see Table 2). The predictions of Ref. 1 indicate 10 to 17 percent lower pressures for combustion gases due to their different thermal properties. Because the prediction of the pressure distribution over Configuration 2 is much more complex than for the cone, additional estimates to isolate the magnitude of some of the effects have not been carried out. However, it is worth noting that the difference between experiment and simple theory as summarized in Tables 1 and 2 was about 5 percent for both body of revolution configurations.

As pointed out in Ref. 1, pressure distributions for bodies such as these may be more nearly matched if one allows the tunnel supply conditions to be different between test media and specified in a manner such that the pressure at the body stagnation point be the same. The effectiveness of this scheme may be observed in Figs. 6b and 7b. When the stagnation point pressures are the same, it appears that pressures may be rather closely matched over the forward portions of the bodies, but that differences existing over the rear portions may cause changes in the pitching moment. Although application of this scheme would be somewhat complicated, it would avoid the use of corrective increments to adjust combustion gas data to approximate air results.

Theoretical predictions of the pressure distributions for the double wedge configuration of Ref. 1 employed the simple inviscid shock-expansion

method accounting for vibrational real gas effects. Since the experimental data (Fig. 8) revealed strong leading edge and viscous interaction effects, an attempt was made to improve the theoretical predictions by incorporating at least the viscous interaction effects as suggested by Lees and Probstein (Ref. 7).

A typical schlieren photograph of Configuration 3 (Fig. 9) shows that curvature of the bow shock extends to the midsection of the wedge. This implies that the tip blunting effect is active at least to the region of the midsection. This effect, in part, accounts for the severe pressure gradients found on the compression surfaces as shown in Fig. 8. The viscous interaction phenomena account for the remaining portion of the pressure gradients.

A comparison of the flow patterns for the wedge at α = 10 deg for both test media is presented in Fig. 10. The thinner boundary layer observed on the wedge during the combustion gas runs would indicate that bodies tested in products of combustion would appear to be smaller to the flow field.

Pressure distributions for Configuration 3 are somewhat irregular particularly at zero angle of attack; however, typical differences indicated between the test media have been summarized in Table 3. The combustion gas test medium produced up to 35 percent lower pressures along the upper wedge surfaces than did air. Over the lower surface the difference between test media was, in general, much less. The theoretical difference between test media which again did not account for water condensation varied widely from surface to surface, and up to 100 percent higher pressures were indicated for combustion gases. The result of these differences is illustrated by a plot of the section lift force in Fig. 11, which was obtained by integrating the local pressure distributions. Greater total lift forces would be experienced at all angles of attack in a combustion gas test medium because the test section static pressure level for combustion gases is greater than in air. If the total lift data (Fig. 11) were expressed in coefficient form, the same trends would exist. This is attributed to the reduction in combustion gas Mach number compensating for the increase in free-stream static pressure as illustrated by the following equation:

$$C_N = \frac{1}{\frac{1}{2}\,\gamma_\infty\, p_\infty\, M_\infty^{\,2}\, A} \int (p_L - p_U)\, dA$$

For the bodies of revolution the simple noncondensing theories predicted pressures about 5 percent lower than found by experiment. This trend did not exist for the two-dimensional wedge, and the direction of

differences were sometimes reversed between experiment and theory (compare Tables 1 through 3). Consequently, it would appear quite difficult to evaluate data obtained for complete configurations in combustion gases. Moreover, the distribution of loading produced by the test media will be different, and pitching moments obtained in a combustion gas test medium will not represent those of air. Thus, in general, combustion gases which would condense in the tunnel nozzle would produce pressure, force, and moment data which would be hard to interpret to actual flight conditions. Furthermore, it does not appear possible to incrementally correct such test data to the case of air by use of present conventional (noncondensing) theories such as employed in Ref. 1.

3.2.2 Heat Transfer Distribution

Since the data obtained at the stagnation point on Configuration 2 were widely scattered, Ref. 2 suggests extrapolating measurements to θ = 30 deg for determining the stagnation point heat transfer rate.

The experimental heat transfer distributions with dry air for Configuration 2 (Fig. 12) agreed with those obtained by other investigators (for example, Ref. 8).

The heat transferred to the flare region on Configuration 2 (referenced to the stagnation point value) was less for combustion gases than for air; whereas, over the hemisphere and cylinder the opposite is true. These trends are summarized in Table 4. Heat transfer data were also obtained with a pseudo-combustion gas containing no water vapor. These data more or less coincide with the results obtained with an air test medium. Consequently, the reversal of the heating rates along the body, which resulted with the wet combustion gases, is thought to be some complicated effect of condensation or re-evaporation.

The theoretical predictions for air and combustion gases (without condensation) are also given in Fig. 12 and Table 4. The Kemp, Rose, and Detra theory (Ref. 8) predicts the experimental trends most accurately over the initial portion of the body, but poor agreement with experiment is found over the remainder of the blunt body surface where uncertainties in the theory exist.

The total heat transferred to Configuration 2 in terms of Btu/sec was obtained by integrating the local heating rates over the entire model surface and is summarized in the table on the following page.

	Total Heat Transferred to Flared Hemispherical Cylinder, Btu/sec	
	Air	Products of Combustion
Theory	116.4	117.4
Experiment	107.4	102.1

Thus, with a combustion gas test medium, Configuration 2 experienced about a 5 percent lower overall heating rate than it did in air. Although the total heating rates of the bodies in the two test media were not significantly different, this should not be interpreted as a justification for the use of combustion gases. Duplication of local heat transfer rates is necessary.

Heat transfer coefficients measured for the double wedge model (Configuration 3) by the transient technique are given in Figs. 13a through 13d. Because of the experimental scatter, about ±15 percent from the mean, it is difficult to draw conclusions from these data. Typical incremental differences between the two test media summarized in Table 5 indicate that in general the combustion gas test medium produced lower heat transfer coefficients than did air. This result is consistent with that found for the blunt body configuration.

Estimates of h by the reference enthalpy method (Ref. 9) which are also shown in Fig. 13 deviate from those presented in Ref. 1 in that the variation of $\rho\mu$ across the boundary layer is considered. This parameter $(\rho^*\mu^*/\rho_\delta\mu_\delta)$ is included to account, in part, for the effects of severe local pressure gradients (blunting and viscous effects) measured over the wedge surfaces. In addition, estimates by the theory recently published by Bertram and Feller (Ref. 10) are also given. Both of these methods do not account for any condensation effects.

Neither Eckert's reference enthalpy method or the Bertram and Feller theory were accurate for predicting the heat transfer coefficients measured in dry air. Although somewhat better estimates were provided by the Bertram and Feller theory, this is due, at least in part, to using measured pressures; whereas the reference enthalpy method was calculated with theoretical inviscid pressures. Some of the difficulty in applying these methods (even for an air testing medium) may lie in correctly interpreting the free-stream conditions of the experimental tests or in the inaccuracies of the experimental data. In any event, it would not be possible to simply predict corrective heat transfer increments to adjust combustion gas results to the case of air.

3.2.3 Resumé of Test Results

All of the experimental data clearly demonstrate that if condensation occurs during the use of a combustion test medium, the test results, such as aerodynamic loading, pitching moments, and thermal loading, will not represent actual flight conditions. If condensation did not occur in the tunnel nozzle but occurred locally over the body, interpretation of test results would be more confused than outlined here because of local condensation shocks. As indicated in Fig. 3, it may be possible by use of higher temperatures and lower pressures to avoid condensation for lower Mach number testing. This however restricts the usefulness of combustion gases to low Mach numbers and introduces new problems associated with non-equilibrium flow, which are discussed in the next section. Moreover, as illustrated by the theoretical estimates given here and in Ref. 1, combustion gases will still produce different test results because of their different thermal and transport properties.*

3.3 EFFECTS OF NON-EQUILIBRIUM FLOW CONDITIONS

3.3.1 Molecular Vibration

In a high-velocity flow, gas molecules which are heated through a strong bow shock may pass the body before they reach vibrational equilibrium. Thus, the gas can be thought of as "frozen", and constant γ compressible flow calculations are valid. On the other hand, if the vibrational excitations occur extremely fast, equilibrium solutions may be employed. For intermediate non-equilibrium flows, no simple treatments are available, and the problem becomes quite complex.

Some estimates of vibrational relaxation times and flow residence times in the stagnation region of Configuration 2 have been made for

---

*A technique is described in Ref. 11 which allows for compensation of the different gas properties of combustion products by adding small amounts of certain other gases to the combustion gas mixture. Experimental tests were carried out in which a mixture of (1) combustion gases (JP-4 and air), (2) argon, (3) helium, and (4) oxygen produced the same results as air for subsonic flow through a tube, while combustion gases alone produced different results. This method is only valid in the lower M_∞ range where condensation will not occur and with room temperature gases added to the combustion gas, will result in simulation of air up to about 3300°R.

typical conditions of the Ref. 2 tests. The average velocity between the bow shock and stagnation point was about 470 ft/sec. With a mean shock stand-off distance (λ = 0.202 in.) indicated by schlieren photographs, the gas residence time in the stagnation region was about 36 microseconds.

The vibrational relaxation time for air at the stagnation point conditions was found from Ref. 12 to be much greater (1,170 microsec) than the residence time available. Thus, in the stagnation region for dry air runs the flow may be treated as "frozen." Vibrational relaxation times for combustion gas mixtures are not available. However, Table 6 lists typical relaxation times for various gases at low temperature and the average number of collisions required to achieve equilibrium. These characteristics aid in understanding the combustion gas vibrational relaxation behavior.

The H_2O and CO_2 components of the combustion gas would reach equilibrium more rapidly than does air. The presence of H_2O or CO_2, however, can have an important effect on the relaxation time for oxygen or nitrogen vibrations, because of the much greater effectiveness of oxygen-water or nitrogen-water molecular collisions compared with oxygen-oxygen or oxygen-nitrogen collisions (see Table 6). For example, at a temperature of 555°R, only about 400 oxygen-water vapor collisions on the average would be necessary to establish vibrational equilibrium for the oxygen component while 10^5 oxygen-nitrogen collisions are needed. References 13 and 14 contain a detailed discussion of this catalytic effect.

A combustion gas should reach the equilibrium state more rapidly than would air, but it is probably still frozen in the stagnation region for the conditions of the Ref. 2 tests.

Mach number estimates made assuming frozen flow were less than one percent greater than those given previously for equilibrium flow (from Ref. 2, Table 4). These small deviations in Mach number would have a negligible effect on the comparisons made by this report.

Thus, it may be concluded that even if air and combustion products have somewhat different vibrational non-equilibrium behavior, the effect on any test results should be minor in the temperature range of this study. However, at higher temperatures these effects would become more pronounced.

3.3.2 Molecular Dissociation

The National Bureau of Standards has calculated the thermodynamic properties and equilibrium compositions of the combustion gas mixture

which results from the combustion of C_2H_4 and air with a fuel-air ratio of 0.06. This combustion gas typically represents the test media of a 4000 to 6000°R combustion heated tunnel.* The equilibrium composition of this gas mixture at a $\rho/\rho_o = 10^{-2}$ is shown in Fig. 14a for various temperatures from 2880°R to 5400°R. Figure 14b gives the equilibrium composition for air at the same conditions (obtained from Ref. 16).

The assumed combustion gas would achieve an equilibrium temperature of about 4000°R with an initial air temperature of 540°R. With preheating or cooling, the temperature and density levels of Fig. 14 correspond to those at the stagnation point of the blunt body configuration for the following flow conditions:

(a) Current Range of Investigation	(b) Typical Range of Combustion Heated Tunnel
$M_\infty = 6.64$	$M_\infty = 6.64$
$T_t = 2880°R$	$T_t = 5400°R$
$Z = 140,000$ ft	$Z = 145,000$ ft
$p_t = 138$ psia	$p_t = 130$ psia

The equilibrium composition of the combustion gas at a temperature of 2600-2880°R (Fig. 14a) is not much different than the composition specified by the chemical equation

$$C_2H_4 + 3.4019O_2 + 12.6545N_2 + 0.0814A \rightarrow$$

$$2CO_2 + 2H_2O + 0.4019O_2 + 12.6545N_2 + 0.0814A$$

Only about 0.1 of one percent of the combustion gas molecules are dissociated. This amount of dissociation is insignificant and would not appreciably affect the theories or account for experimental inconsistencies presented in this report.

At a temperature of 5400°R, however, most of the H_2O and CO_2 molecules would be dissociated as would a few percent of the N_2. The amount of molecular O_2 increases (opposite to the behavior of air) presumably because of the O_2 freed by CO_2 and H_2O dissociation. Also, about 8 percent by volume of H_2 and H would be formed. Because of the extreme gas properties of H_2 and H, the formation of these two gases would significantly modify the combustion gas properties. Moreover, about 28 percent by volume of the combustion gas is now dissociated compared to about 10 percent for air.

*The reference is to tunnels which incorporate combustion gases as the test medium.

To dissociate the amount of N_2 and O_2 which would occur in air (Fig. 14b) requires an energy of about 875 Btu per lbm of air. This is surprisingly close to the 825 Btu per lbm of combustion gases needed to cause the degree of dissociation of N_2, CO_2, and H_2O indicated in Fig. 14a for combustion gases. As a reference, the enthalpy of air at $T = 5400°R$ and $\rho/\rho_o = 10^{-2}$ is about 3300 Btu/lbm.

Although the energy involved in dissociating the various gas species in air and combustion gases is not significantly different at the higher temperatures, the combustion gas mixture would have greatly different thermal and transport properties and a different distribution of energies. Consequently, in the high temperature range of combustion heated tunnels, it is questionable whether combustion gases can produce the same test results as would air even if condensation can be avoided. These effects would be somewhat more pronounced if fuels with higher hydrogen-carbon ratios are used because of the larger amount of H_2O formed during combustion.

3.4 TESTING AND OPERATING DIFFICULTIES

Additional problems associated with the use of combustion gases may be expected during tunnel operation.

Combustion processes occurring either in or upstream of the stagnation chamber may increase the general turbulence level of the flow entering the nozzle, resulting in a change of the "aerodynamic" noise level within the test section. The unsteady nature of combustion may also result in severe pressure, temperature, and velocity gradients in the test section.

If the combustion efficiency is less than 100 percent, the possibility of free carbon (soot) exists. Conceivably, the carbon could affect data dependent upon local skin friction values and any instrumentation exposed to free-stream conditions. Some unpublished AEDC tests indicate that soot deposits may be severe in regions where the flow is rapidly expanded to low temperature.

4.0 CONCLUDING REMARKS

The prime considerations in evaluating products of combustion as an aerodynamic test medium are: (1) if test results obtained in combustion products can be interpreted or corrected to apply to the case of air,

and (2) if the differences are small enough to be neglected. For the bodies included in this investigation, one could not have adjusted the combustion gas test results to predict results measured in air by applying common theoretical methods. For the flow conditions of this study ($M_\infty \approx 6.5$, $p_t = 130$ psia, and $T_t = 2600°R$), the aerodynamic and heat transfer differences produced by a combustion gas test medium in most cases were large enough to affect nearly all development-type tests.

In the present investigation water vapor in the products of combustion condensed during the nozzle expansion and was found to provide the greatest influence on test results. Some of these effects were directly reflected in the interpretation of the test section conditions. In general, test data obtained with air containing similar amounts of water as the combustion gases produced similar effects, whereas dry combustion gas data tended to agree with dry air results. Comparison of test results measured in the various test media conclusively demonstrated the influence of water condensation. Also, because of the large water content of combustion gases, little supersaturation could be expected with its use.

The present test results indicate that a heat transfer test in combustion gases would produce lower total heating rates than would air; however, the local heating rates in general produce much larger differences with a reversal in trends. With respect to aerodynamic loading, different trends were exhibited by different bodies; as a result it would appear that test results obtained in combustion gases for complete wing-body configurations would be extremely difficult to interpret to an air test medium. Also, a combustion gas test medium would produce different body pitching moments.

Non-equilibrium flow effects are at present difficult to apply to the flow of air. The situation becomes much more complex with a combustion gas test medium because of the existence of polyatomic components or if condensation occurs over the test model.

In the range covered by this study, the use of combustion gases as a test medium does not appear promising primarily because of condensation effects of water vapor. If high enough temperatures are employed to avoid condensation, then vibrational and dissociation non-equilibrium flow problems become important and will limit the uses of combustion gases. At present, combustion gases might produce usable results only in some limited intermediate range or in obtaining gross structural effects.

REFERENCES

1. Tempelmeyer, K. E., Nesbitt, M. H., and Carpenter, L. R. "Theoretical Predictions of Inviscid Pressure Distribution and Heat Transfer Rates over Simple Bodies in Air and Combustion Gas Test Media at Hypersonic Speeds." AEDC-TN-60-207, March 1961.

2. Hermann, R., Thompson, K. O., and Melnik, W. L. "Aerodynamic and Heat Transfer Characteristics of Basic Bodies in Hypersonic Flow of Air and of Combustion Gas Mixtures." AEDC-TDR-62-89, April 1962.

3. Strike, W. T. and Norden, B. "Flow Properties of an Unyawed 10° Cone for γ = 1.28 to 1.40 at Mach Numbers of 1.5 to 8.0." AEDC-TN-60-178, October 1960.

4. Stepchkov, A. A. "Condensation Shocks in a Supersonic Nozzle." American Rocket Society Journal, Vol. 30, No. 7, p 695, July 1960.

5. Lewis, C. H. "Pressure Distribution and Shock Shape over Blunted Slender Cones Between M = 16 and M = 19." AEDC-TN-61-81, August 1961.

6. Cheng, H. K., Hall, J. G., Golian, T. C., and Hertzberg, A. "Boundary Layer Displacement and Leading Edge Bluntness Effects in High Temperature Hypersonic Flow." IAS Paper No. 60-38, January 1960.

7. Lees, Lester, and Probstein, Ronald F. "Hypersonic Viscous Flow over a Flat Plate." AD 195, ATI 148565, 1952.

8. Kemp, Nelson H., Rose, Peter H., and Detra, Ralph W. "Laminar Heat Transfer Around Blunt Bodies in Dissociated Air." Journal of the Aero/Space Sciences, Vol. 26, No. 7, pp 421-430, July 1959.

9. Eckert, E. R. G., and Drake, R. M. Heat and Mass Transfer. McGraw-Hill Book Company, Inc., New York, 1959.

10. Bertram, Mitchell H. and Feller, William V. "A Simple Method of Determining Heat Transfer, Skin Friction, and Boundary Layer Thickness for Hypersonic Laminar Boundary Layer Flows in a Pressure Gradient." NASA Memo 5-24-59L, June 1959.

11. Tempelmeyer, K. E., Nesbitt, M. H., and Shepard, J. E. "Simulation of High Temperature Air for Aerodynamic and Heat Transfer Test Purposes." AEDC-TDR-62-40, January 1962.

12. Stephenson, Jack D. "A Technique for Determining Relaxation Times by Free Flight Tests of Low Fineness Ratio Cones; with Experimental Results for Air at Equilibrium Temperatures up to 3440°K." NASA TN D-327, September 1960.

13. Bethe, H. A. and Teller, E. "Deviation from Thermal Equilibrium in Shock Waves." Ballistic Research Laboratory, Aberdeen Proving Ground, Report X-117, 1945.

14. Griffith, Wayland. "Vibrational Relaxation Time in Gases." Journal of Applied Physics, Vol. 21, pp 1319-1325, December 1950.

15. Sedney, R. "Some Aspects of Non-Equilibrium Flows." IAS Paper No. 60-4, January 1960.

16. Hilsenrath, Joseph, Klein, Max, and Woolley, Harold W. "Tables of Thermodynamic Properties of Air Including Dissociation and Ionization from 1500°K to 15,000°K." AEDC-TR-59-20, December 1959.

APPENDIX I

Experimental pressure and heat transfer rate distributions were measured and are given in Ref. 2 for the following combinations of models and test media:

PRESSURE DATA

Model		Test Medium
Flared-Hemispherical-Cylinder	$\alpha = 0°$	Air $\Omega = 0$ Combustion Gas, $\Omega = 0.042$
Cone	$\alpha = 0°$	Air $\Omega = 0$ Air $\Omega = 0.042$ Combustion Gas $\Omega = 0.042$
Wedge	$\alpha = 0°$	Air $\Omega = 0$ Combustion Gas $\Omega = 0$ Combustion Gas $\Omega = 0.021$ Combustion Gas $\Omega = 0.042$
Wedge	$\alpha = 5°$	Air $\Omega = 0$ Combustion Gas $\Omega = 0.042$
Wedge	$\alpha = 10°$	Air $\Omega = 0$ Combustion Gas $\Omega = 0$ Combustion Gas $\Omega = 0.021$ Combustion Gas $\Omega = 0.042$
Wedge	$\alpha = 15°$	Air $\Omega = 0$ Combustion Gas $\Omega = 0.042$

HEAT TRANSFER DATA

Model		Test Medium
Flared-Hemispherical-Cylinder	$\alpha = 0°$	Air $\Omega = 0$ Combustion Gas $\Omega = 0$ Combustion Gas $\Omega = 0.042$

Model		Test Medium
Wedge	$\alpha = 0°$	Air $\Omega = 0$ Combustion Gas $\Omega = 0$ Combustion Gas $\Omega = 0.021$ Combustion Gas $\Omega = 0.042$
Wedge	$\alpha = 5°$	Air $\Omega = 0$ Combustion Gas $\Omega = 0.042$
Wedge	$\alpha = 10°$	Combustion Gas $\Omega = 0$ Combustion Gas $\Omega = 0.021$ Combustion Gas $\Omega = 0.042$
Wedge	$\alpha = 15°$	Air $\Omega = 0$ Combustion Gas $\Omega = 0.042$

TABLE 1

PERCENTAGE DIFFERENCE IN THE PARAMETER, p_ℓ/p_∞, FOR THE 10-DEG HALF-ANGLE BLUNTED CONE, $\alpha = 0$ deg

$$\frac{(p_\ell/p_\infty)_{\text{dry air}} - (p_\ell/p_\infty)_{\text{gas}}}{(p_\ell/p_\infty)_{\text{dry air}}} \times 100$$

	Gas	Conical		Base	Average over Conical Surface
		x/D = 0.073	x/D = 2.20		
Experiment	Combustion Gas, $\Omega = 0.042$	+16	+19	+18	+15
	Air, $\Omega = 0.042$	+20	+20	+15	+19
Theory*	Combustion Gas, $\Omega = 0.042$	+10	+10		+10
	Combustion Gas, $\Omega = 0$	+8	+8		+8

*Water in vapor state.

TABLE 2

PERCENTAGE DIFFERENCE IN THE PARAMETER, p_ℓ/p_∞, FOR THE FLARED HEMISPHERICAL CYLINDER, $\alpha \approx 0$ deg

$$\frac{(p_\ell/p_\infty)_{\text{dry air}} - (p_\ell/p_\infty)_{cg}}{(p_\ell/p_\infty)_{\text{dry air}}} \times 100$$

(Combustion Products, $\Omega = 0.042$)

EXPERIMENT	HEMISPHERE		CYLINDER	FLARE	
	S/R = 0.78	S/R = 1.25	S/R = 3.55	S/R = 6.3	S/R = 9.3
p_ℓ/p_∞	+16	+16	+16	+18	+20
THEORY*	Newtonian	Prandtl–Meyer	Blast Wave	Faired	Conical Theory
p_ℓ/p_∞	+15	+17	+12	+10	+10

*Water in vapor state.

TABLE 3

PERCENTAGE DIFFERENCE IN THE PARAMETER, p_ℓ/p_∞, FOR THE 6-deg HALF-ANGLE DOUBLE WEDGE

$$\frac{(p_\ell/p_\infty)_{\text{dry air}} - (p_\ell/p_\infty)_{cg}}{(p_\ell/p_\infty)_{\text{dry air}}} \times 100$$

(Combustion Products, $\Omega = 0.042$)

Angle of Attack, α, deg		Upper Surface		Lower Surface	
		Front	Rear	Front	Rear
0	Experiment	+24	+6	**	**
	Theory*	+9	+23	+9	+23
5	Experiment	+18	+18	+4	-2
	Theory*	+14	+35	+13	+29
10	Experiment	+12	+21	+3	+11
	Theory*	+11	-60	+13	+20
15	Experiment	+24	+35	+10	+17
	Theory*	+16	-100	+14	+25

*Water in vapor state.

**Insufficient data

TABLE 4

PERCENTAGE DIFFERENCE IN HEAT TRANSFER RATES $(\dot{q}/\dot{q}_o)$ FOR THE FLARED HEMISPHERICAL CYLINDER, $\alpha = 0$ deg

$$\frac{(\dot{q}/\dot{q}_o)_{\text{dry air}} - (\dot{q}/\dot{q}_o)_{cg}}{(\dot{q}/\dot{q}_o)_{\text{dry air}}} \times 100$$

(Combustion Products, $\Omega = 0.042$)

	HEMISPHERE		CYLINDER	FLARE	
	S/R = 0.78	S/R = 1.30	S/R = 3.65	S/R = 6.70	S/R = 8.75
Experiment	−6	−20	−22	+10	+27
Theory*	Ref. 8 −4	Ref. 8 −10	Ref. 8 −13	Ref. 10 −4	Ref. 10 −4

*Water in vapor state.

TABLE 5

PERCENTAGE DIFFERENCE IN THE HEAT TRANSFER COEFFICIENT, h, FOR THE 6-deg HALF-ANGLE DOUBLE WEDGE

$$\frac{h_{\text{dry air}} - h_{cg}}{h_{\text{dry air}}} \times 100$$

(Combustion Products, $\Omega = 0.042$)

Angle of Attack, α, deg	Data	Upper Surface		Lower Surface	
		Front	Rear	Front	Rear
0	Experiment	+20	+10	+24	+30
	Bertram & Feller } Theory*	+7	+2	+7	+2
	Reference Enthalpy } Theory*	−21	−23	−21	−23
5	Experiment	+34	+41	−26	−42
	Bertram & Feller } Theory*	−21	+10	−15	+1
	Reference Enthalpy } Theory*	−36	−20	−29	−22
10	NO AIR DATA IS AVAILABLE FOR COMPARISON WITH COMBUSTION PRODUCTS.				
15	Experiment	−8	+35 to −38	+17	+9
	Bertram & Feller } Theory*	−19	+22	−2	+15
	Reference Enthalpy } Theory*	−38	−20	−15	−22

*Water in vapor state.

TABLE 6

VIBRATIONAL RELAXATION CHARACTERISTICS FOR VARIOUS GASES AT LOW TEMPERATURES AND ONE ATMOSPHERE

Type Collision	Average Number of Collisions to De-activate a Vibrating Molecule	Vibrational Relaxation Time, sec
$O_2 - O_2$	> 500,000	1000×10^{-6}
$N_2 - N_2$	–	6000×10^{-6}
$H_2O - H_2O$	400	0.37×10^{-6}
$CO_2 - CO_2$	50,000	7×10^{-6}
$O_2 - N_2$	100,000	–
$O_2 - CO_2$	25,000	–
$O_2 - H_2O$	400	–
$N_2 - H_2O$	1,300	–
$CO_2 - H_2O$	105	–

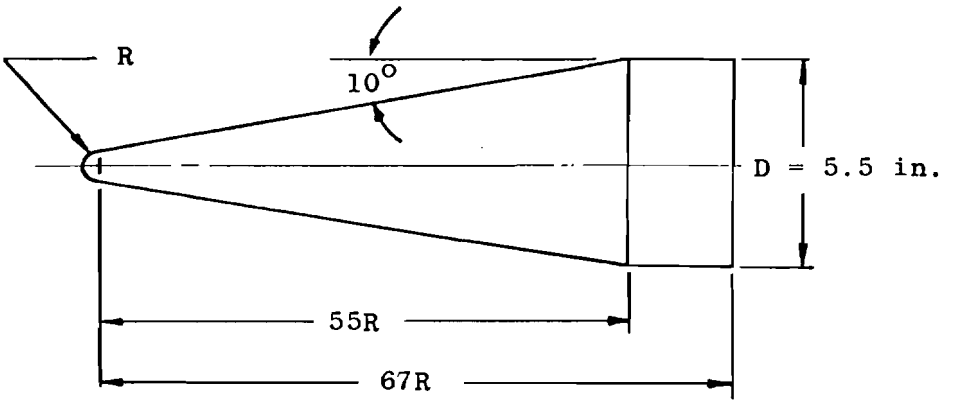

Configuration 1

Geometry of 10-deg Half-Angle Blunted Cone Model, R = 0.25 in.

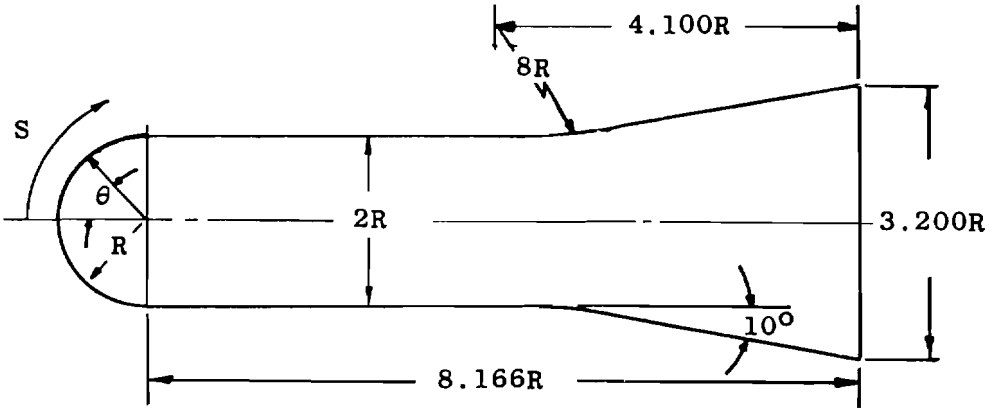

Configuration 2

Geometry of Flared Hemispherical Cylinder Model, R = 1.5 in.

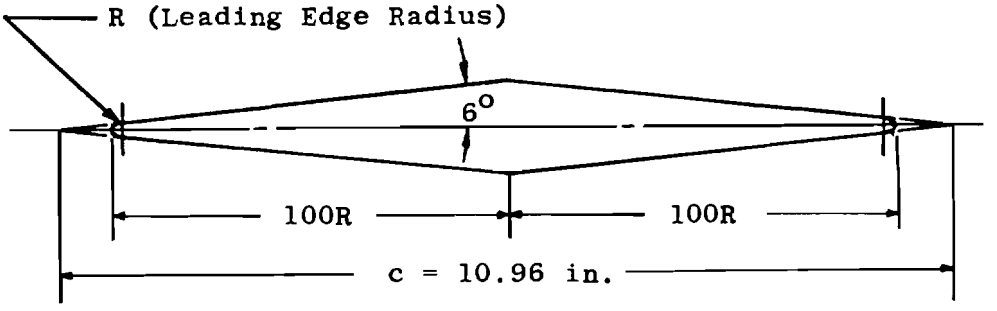

Configuration 3

Geometry of Blunted 6-deg Half-Angle Double Wedge Model, R = 0.25 in.

Fig. 1 Geometric Characteristics of Bodies

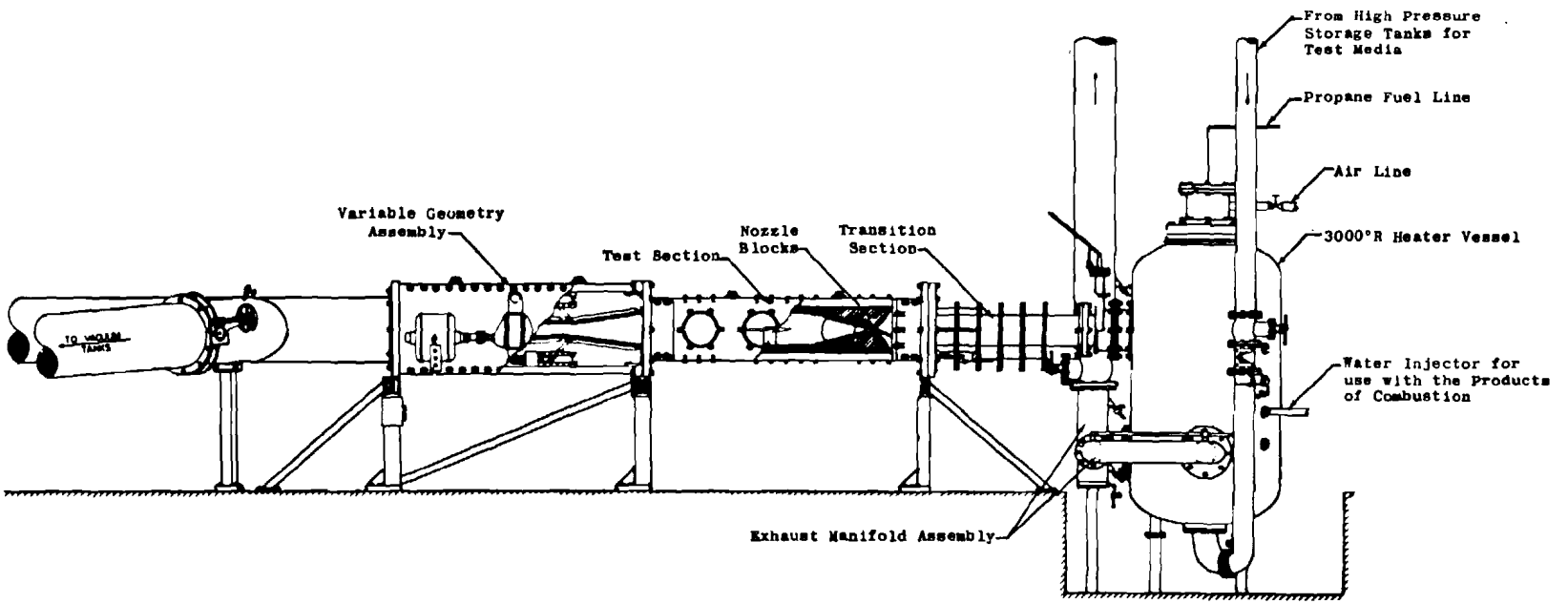

Fig. 2 Schematic of the Hypersonic Blowdown Wind Tunnel, Test Section 12 by 12 in., Rosemount Aeronautical Laboratory, University of Minnesota

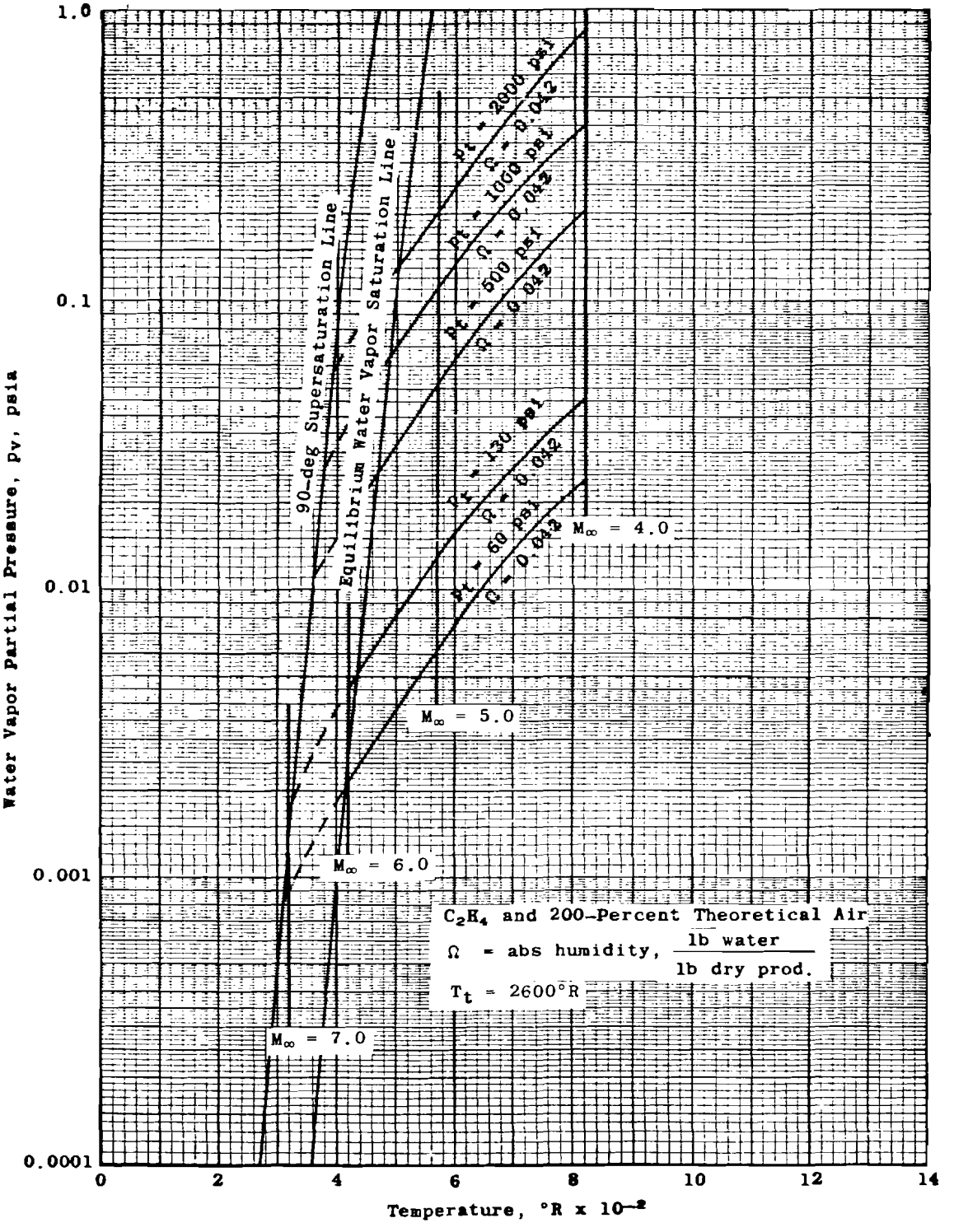

Fig. 3 Partial Pressure of Water Vapor in an Isentropic Nozzle

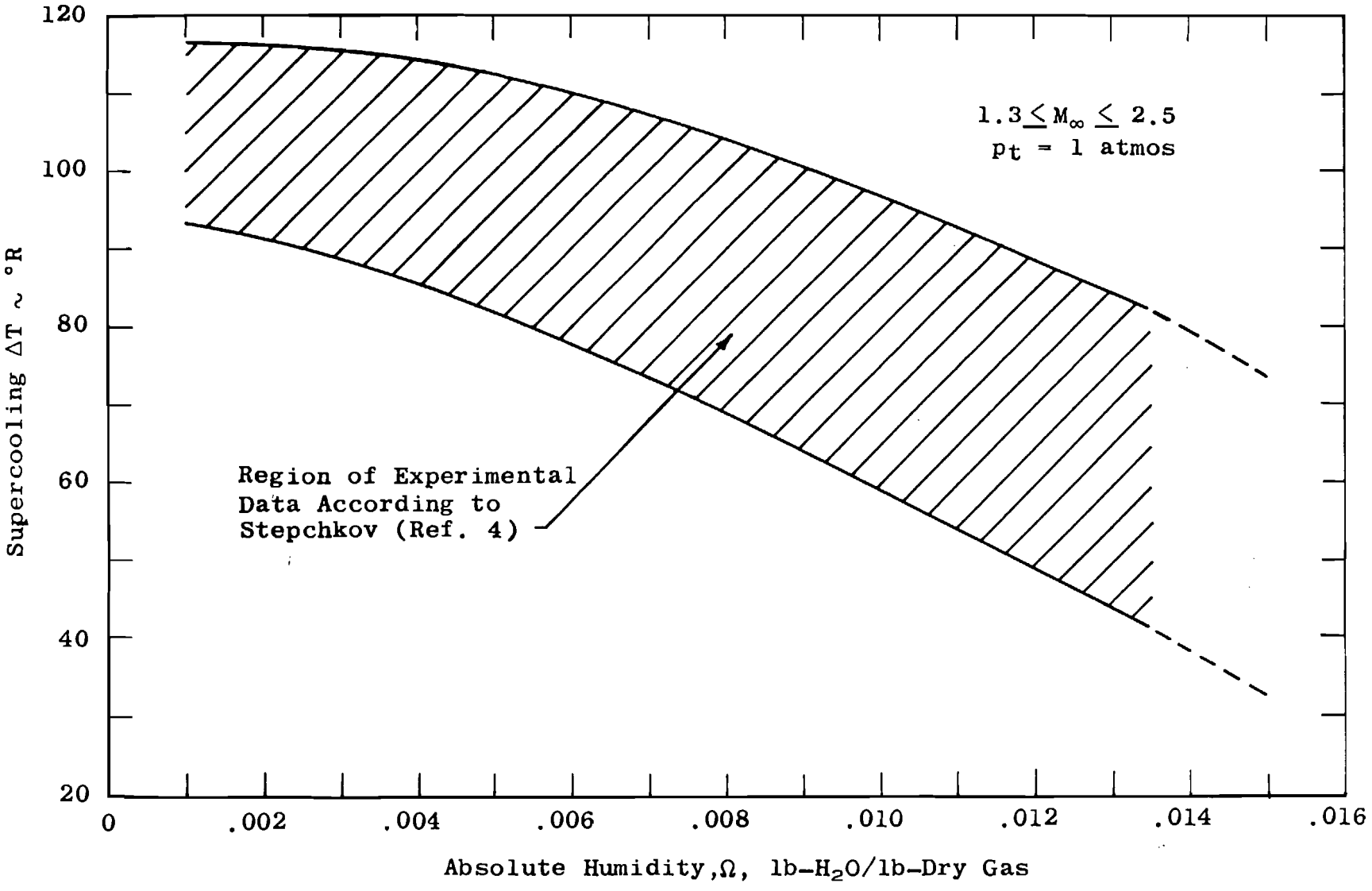

Fig. 4 Wind Tunnel Water Vapor Supersaturation Characteristics as Given by Ref. 4

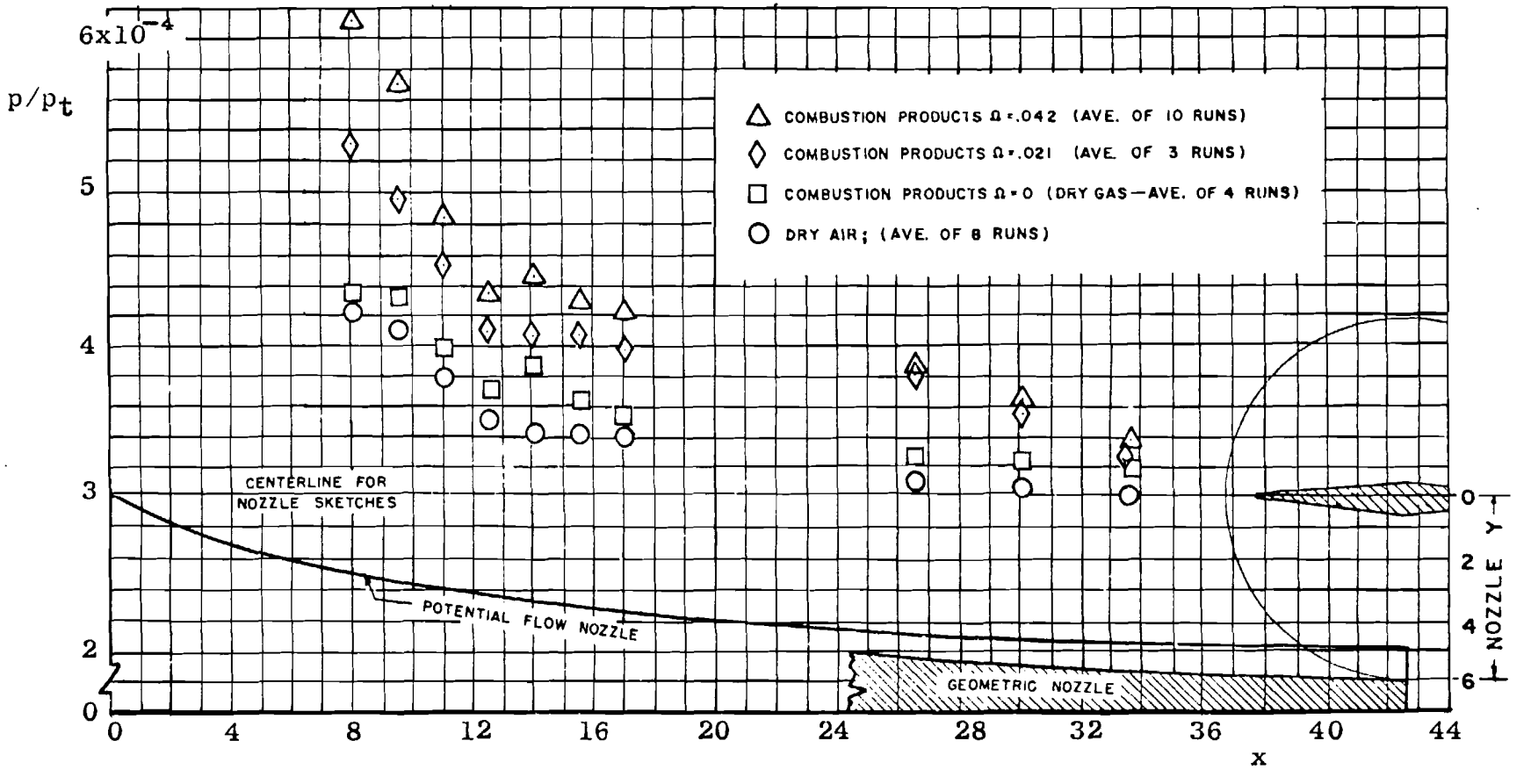

Fig. 5 Tunnel Sidewall Centerline Static Pressure Distributions

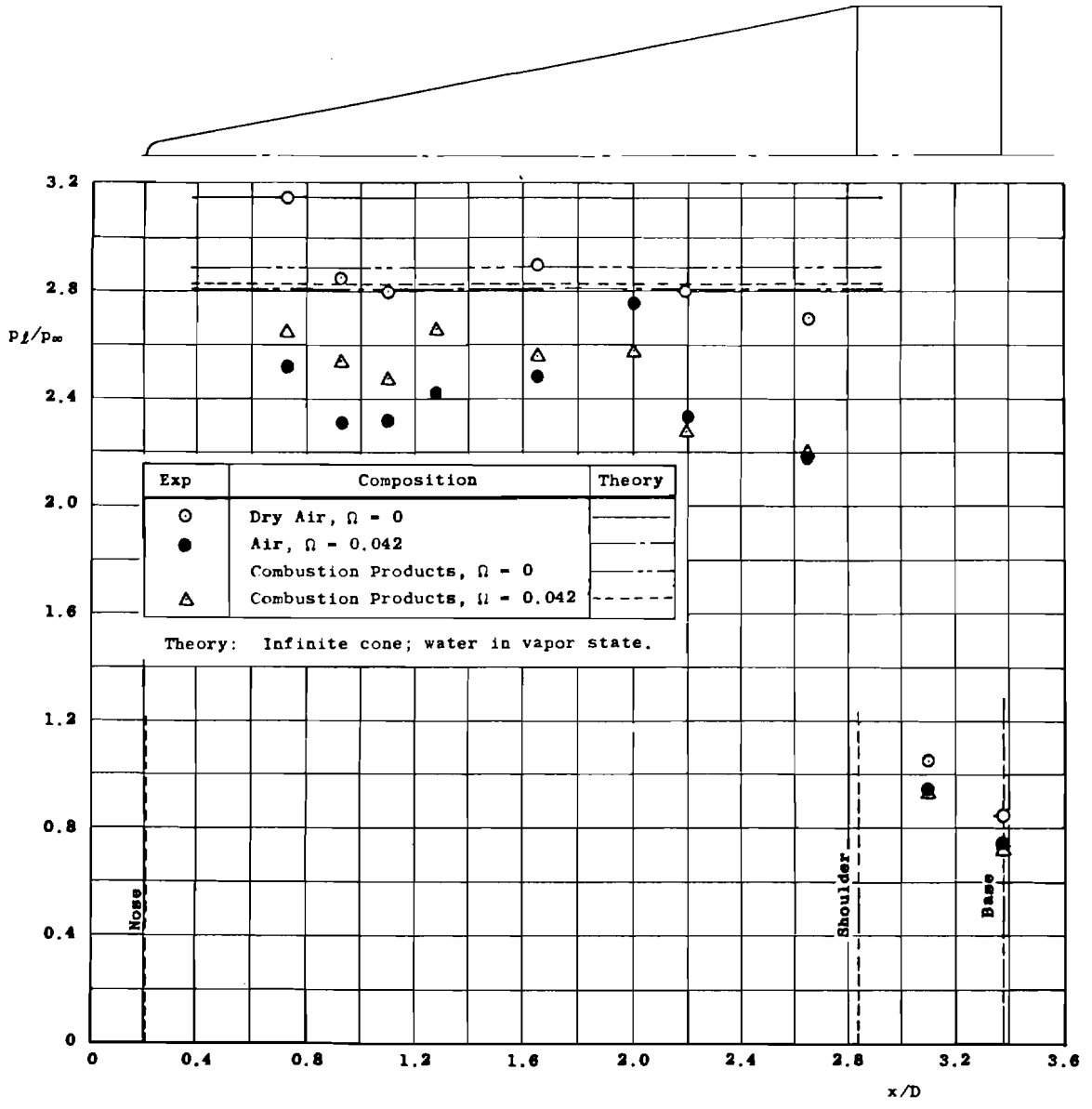

a. p_ℓ/p_∞

Fig. 6 Pressure Distribution on a 10-deg Half-Angle Blunted Cone, α = 0 deg

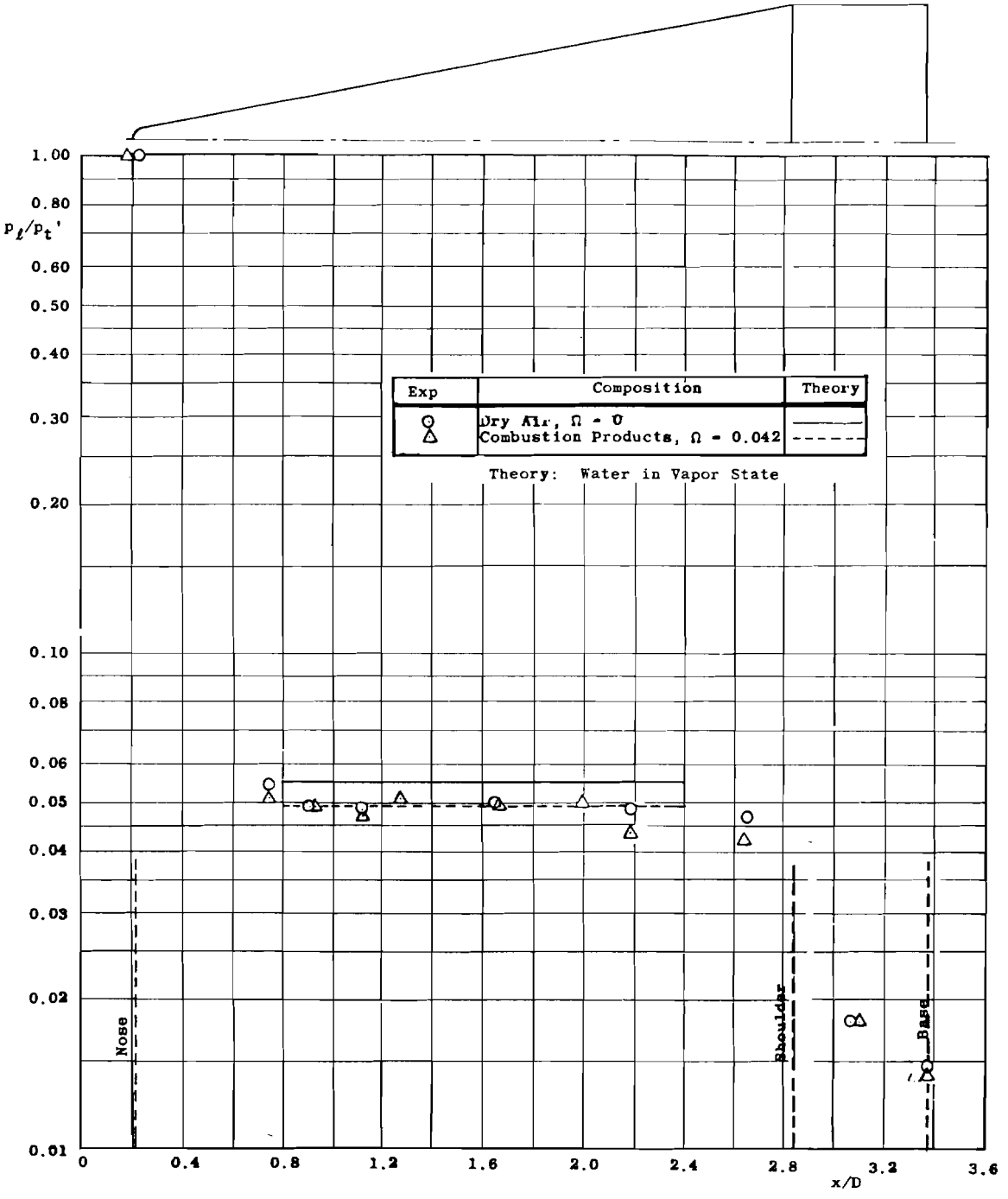

b. p_ℓ/p_t'

Fig. 6 Concluded

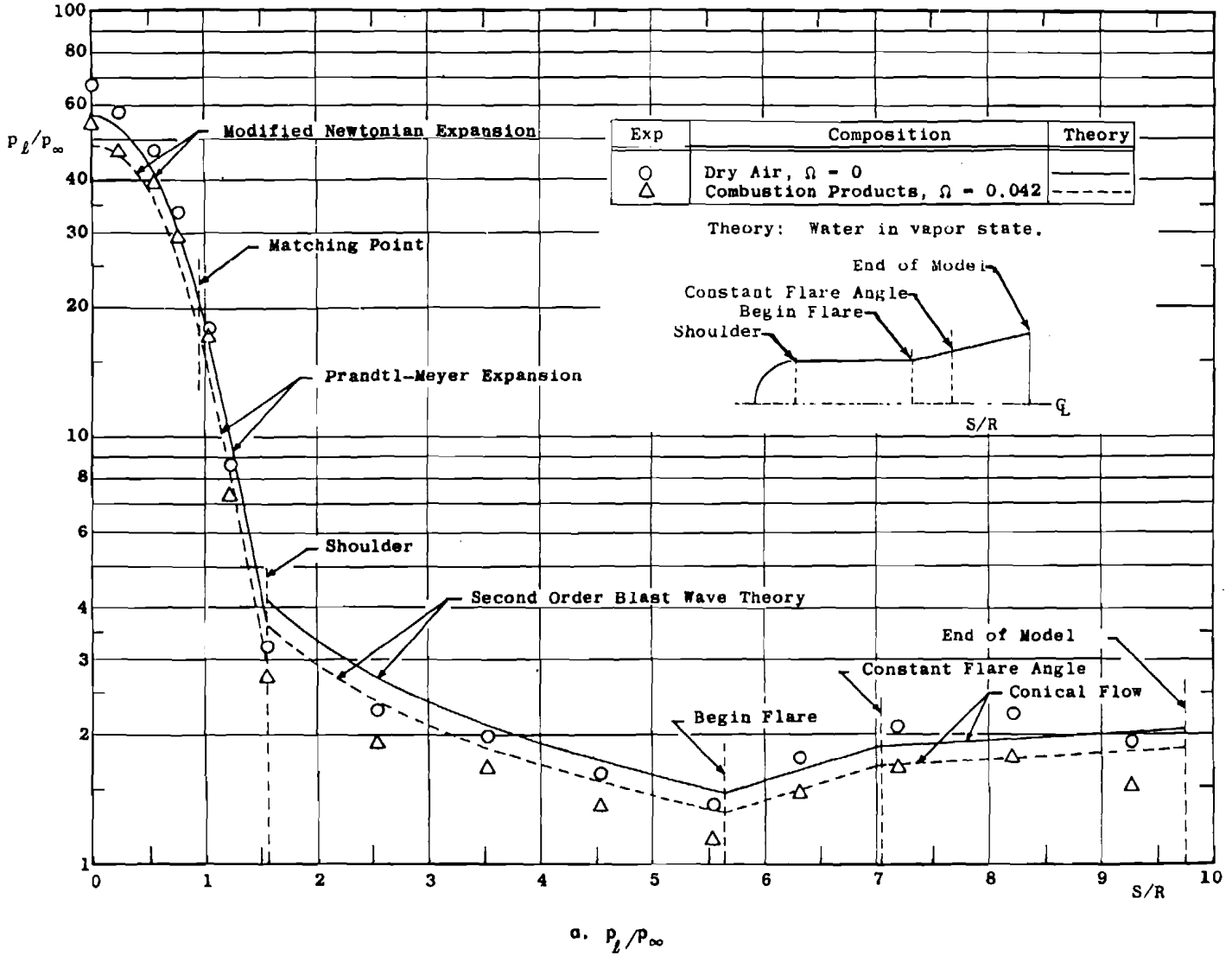

a. p_ℓ/p_∞

Fig. 7 Pressure Distribution on the Flared Hemispherical Cylinder, α = 0 deg

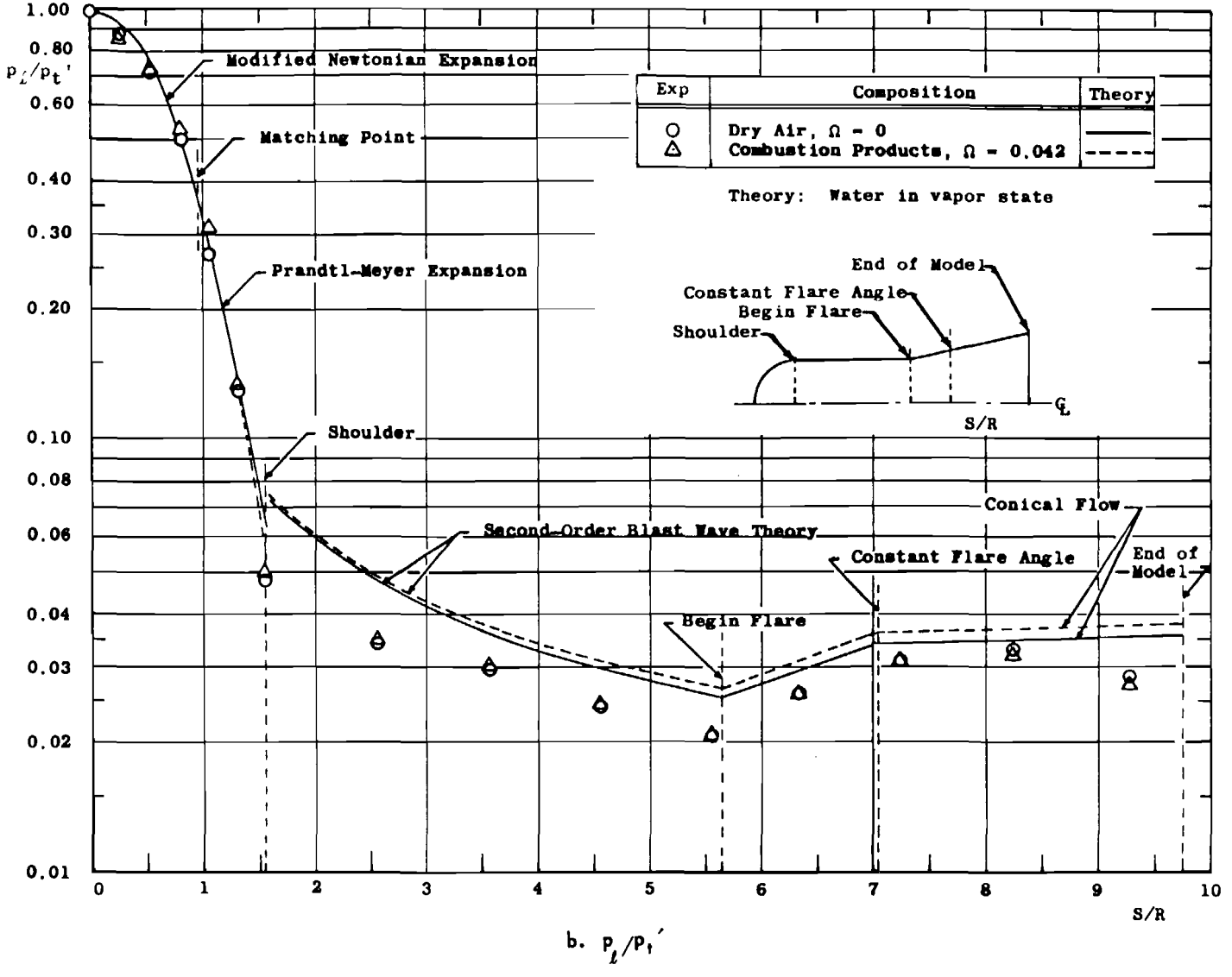

b. p_l/p_t'

Fig. 7 Concluded

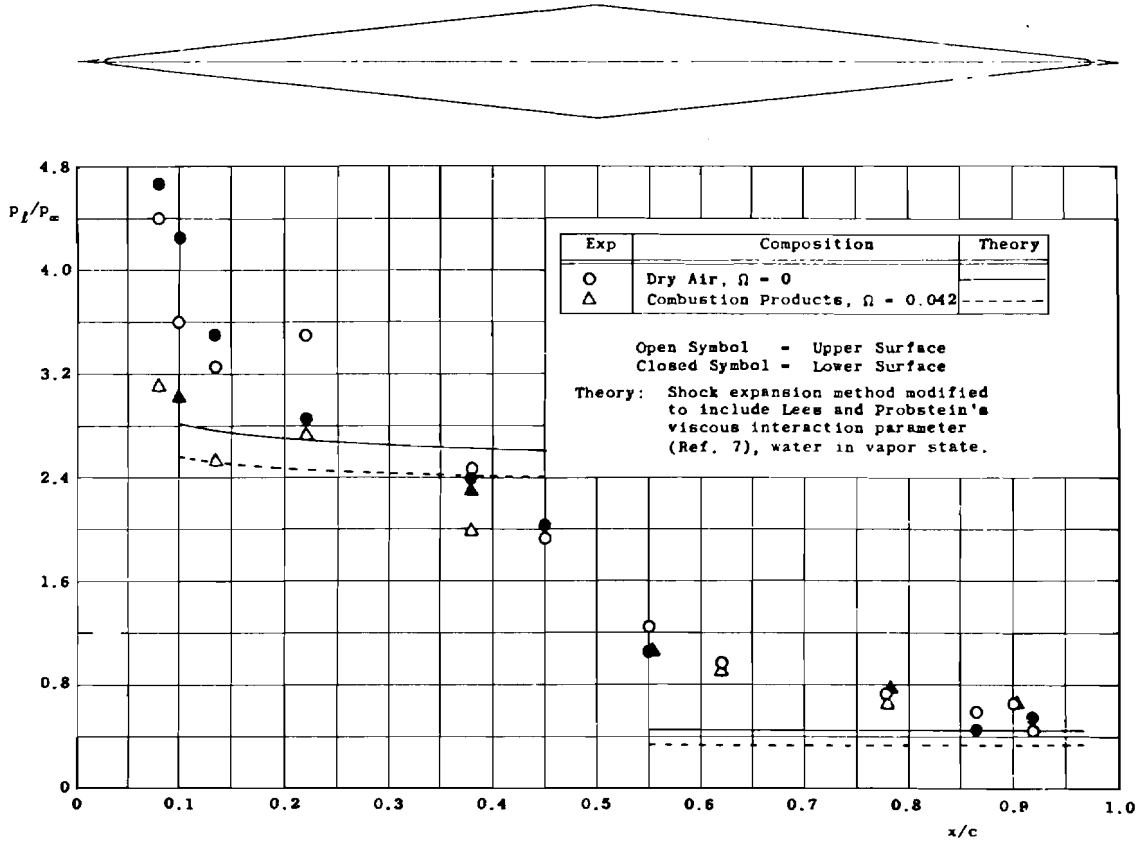

a. α = 0 deg

Fig. 8 Pressure Distribution, p_l/p_∞, on a Blunted 6-deg Half-Angle Double Wedge

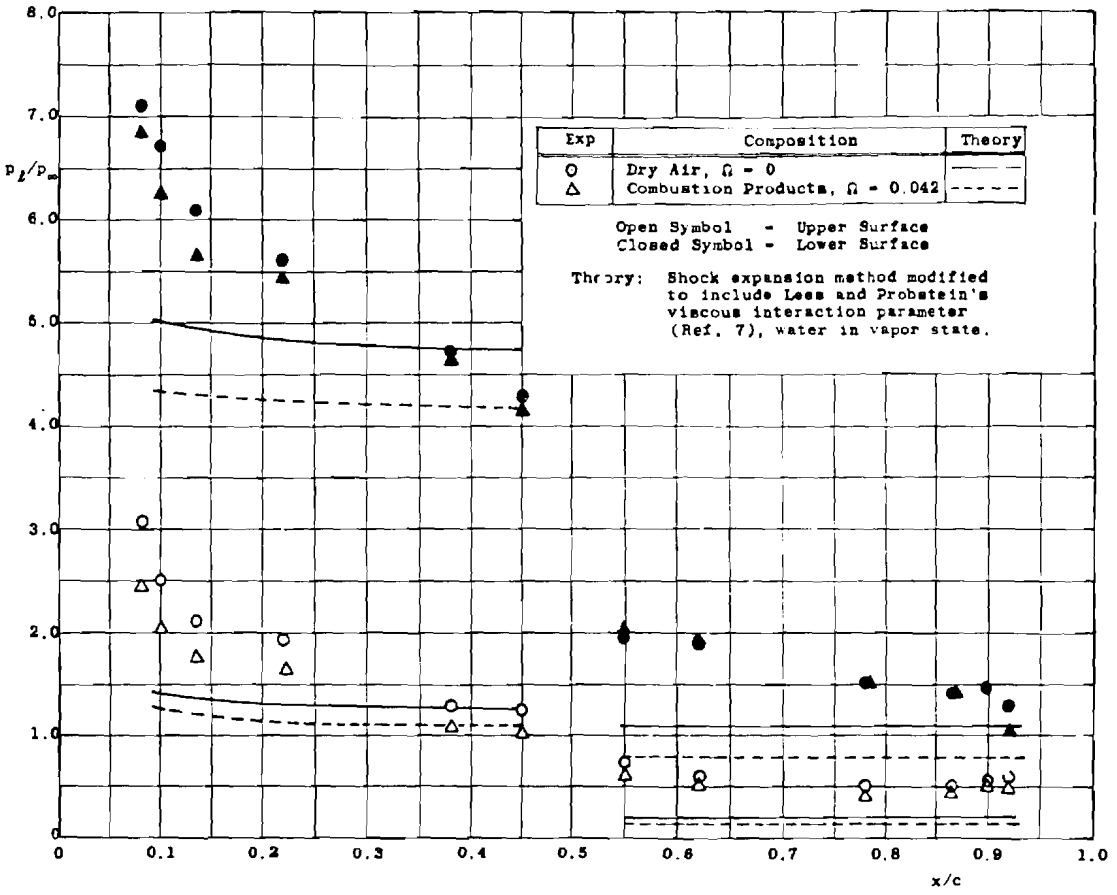

b. $\alpha = 5$ deg

Fig. 8 Continued

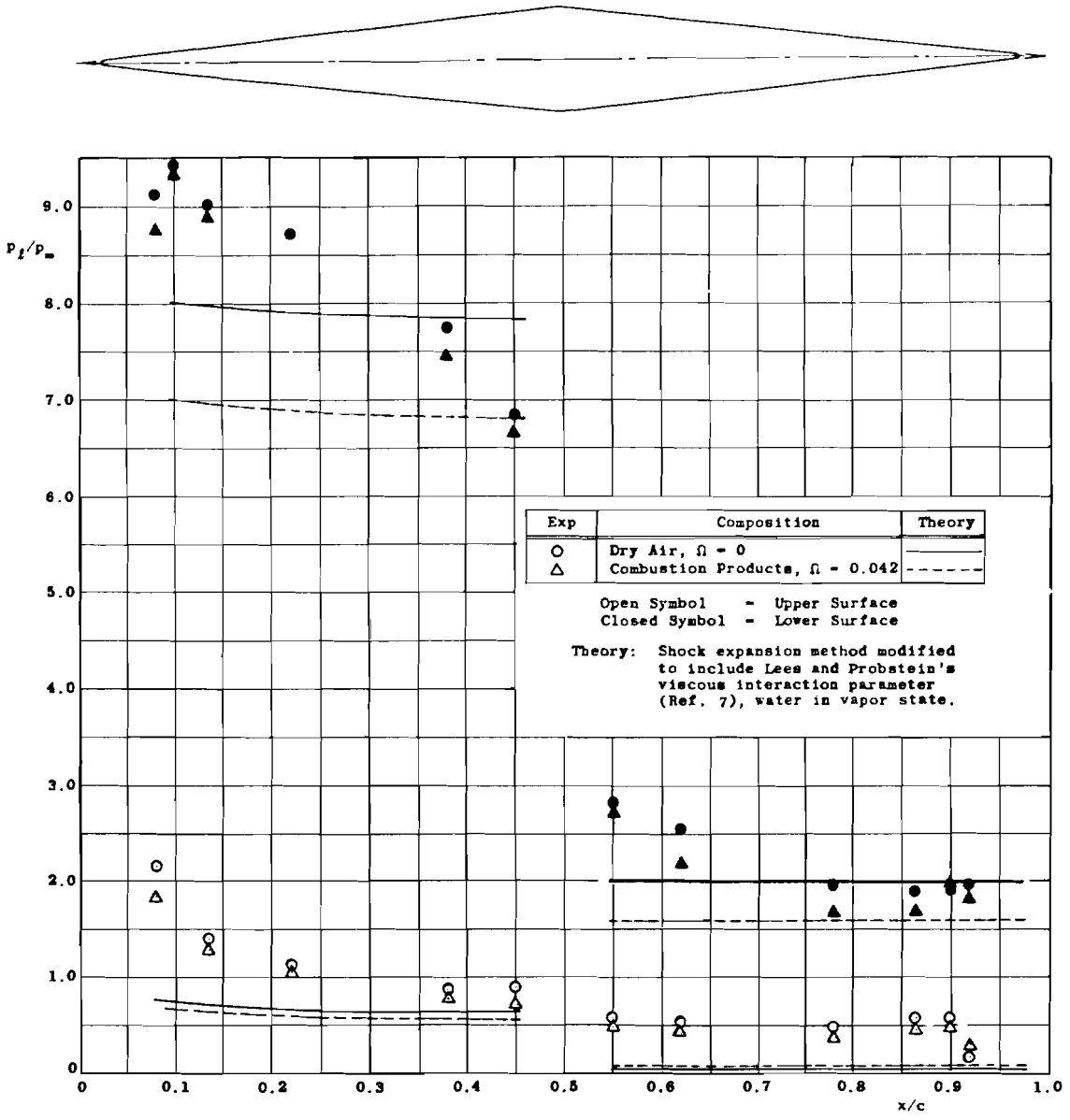

c. $\alpha = 10$ deg

Fig. 8 Continued

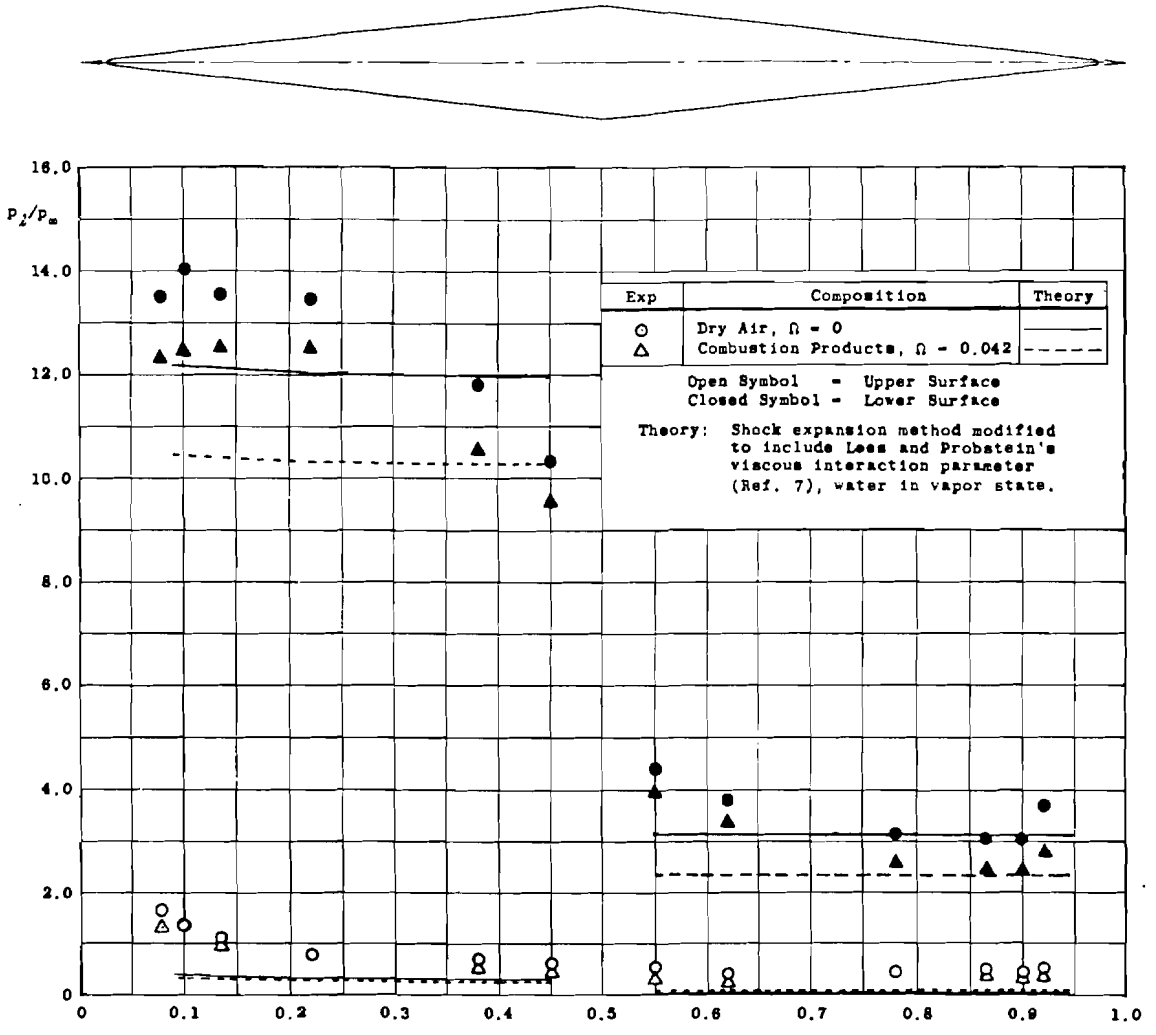

d. α = 15 deg

Fig. 8 Concluded

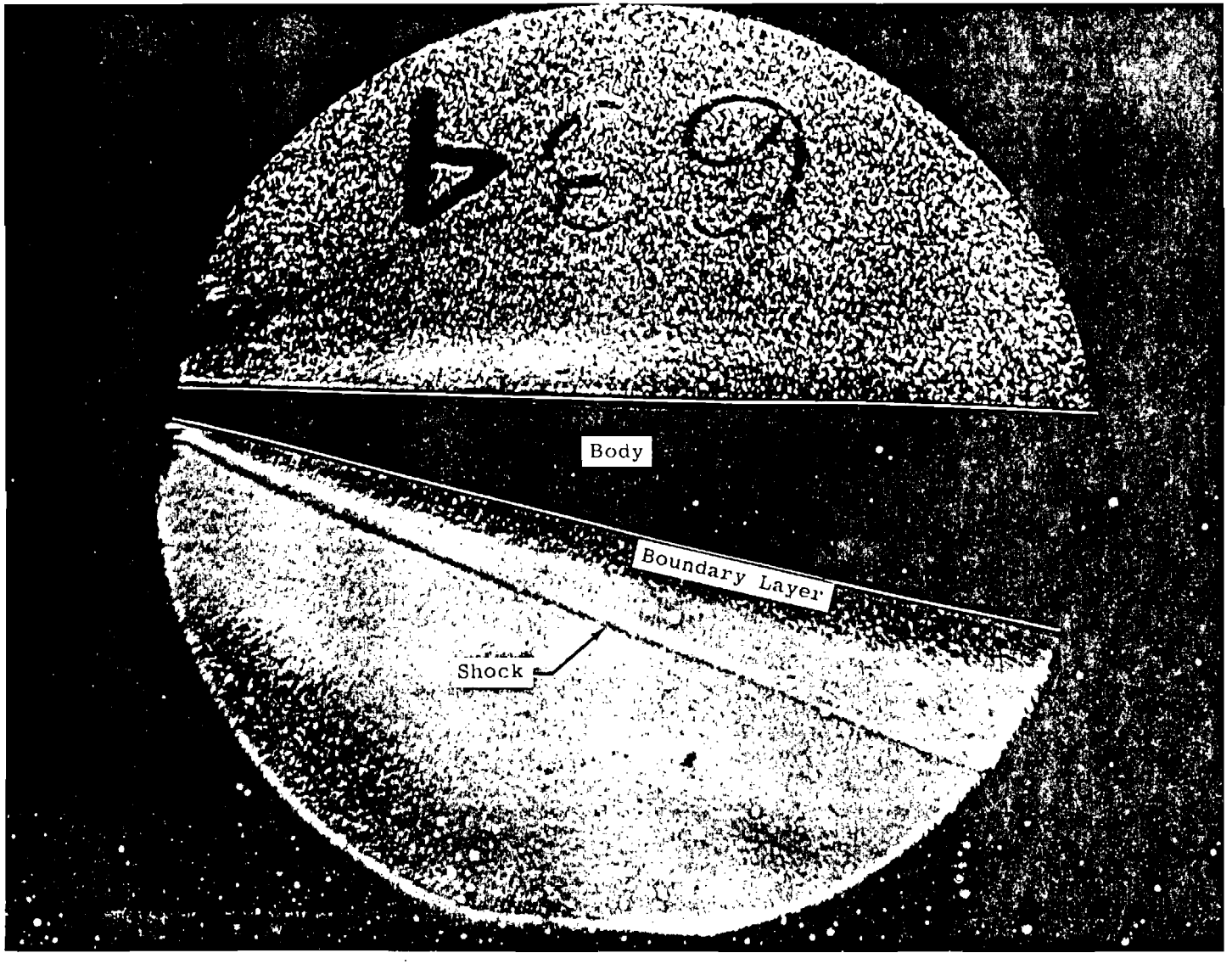

Fig. 9 Schlieren Photograph of Blunted 6-deg Half-Angle Double Wedge, Dry Air, p_t = 130 psia, T_t = 2600°R, α = 10 deg

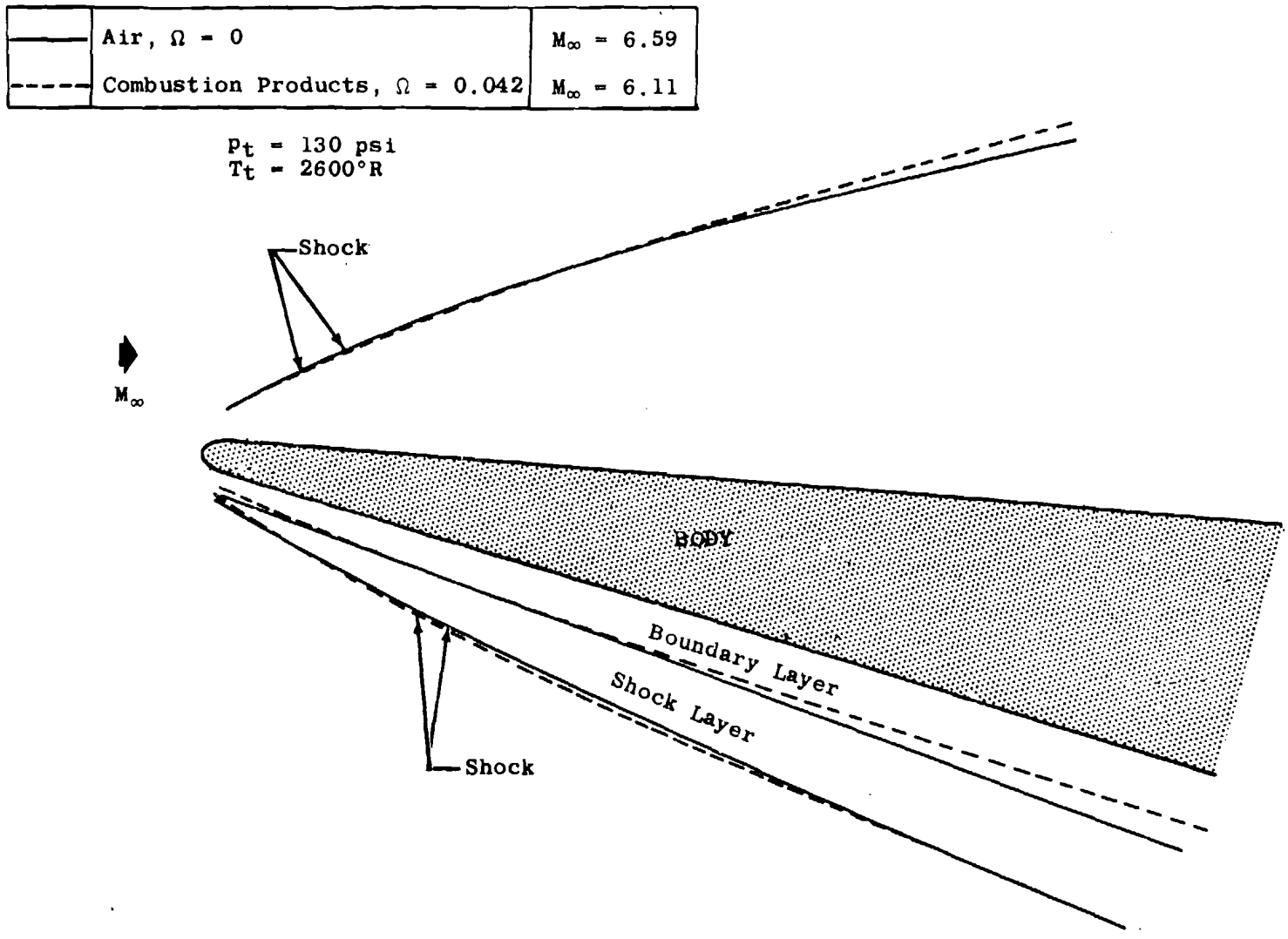

Fig. 10 Comparison of Wave Patterns Between Air and Combustion Gas on a Blunted 6-deg Half-Angle Double Wedge, α = 10 deg

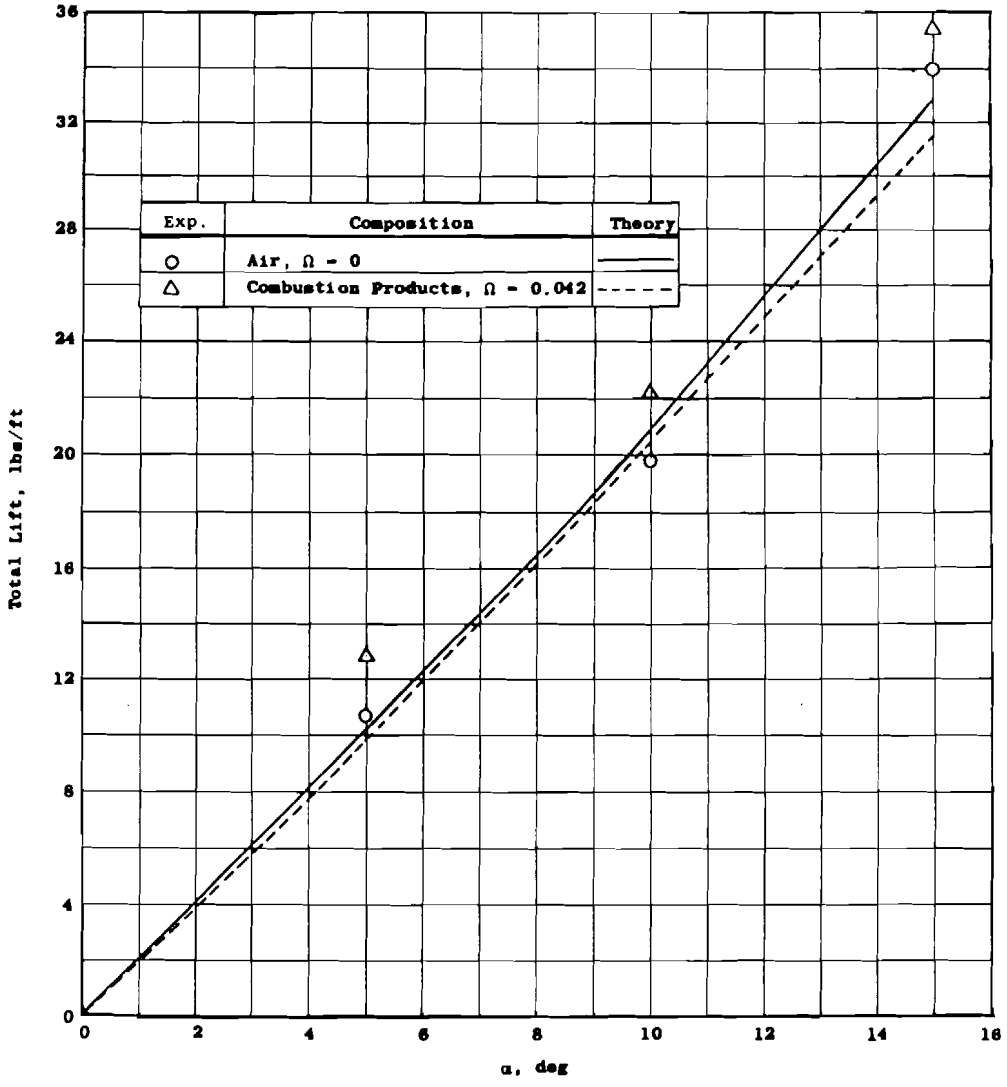

Fig. 11 Lift as a Function of Angle of Attack for the Blunted 6-deg Half-Angle Double Wedge

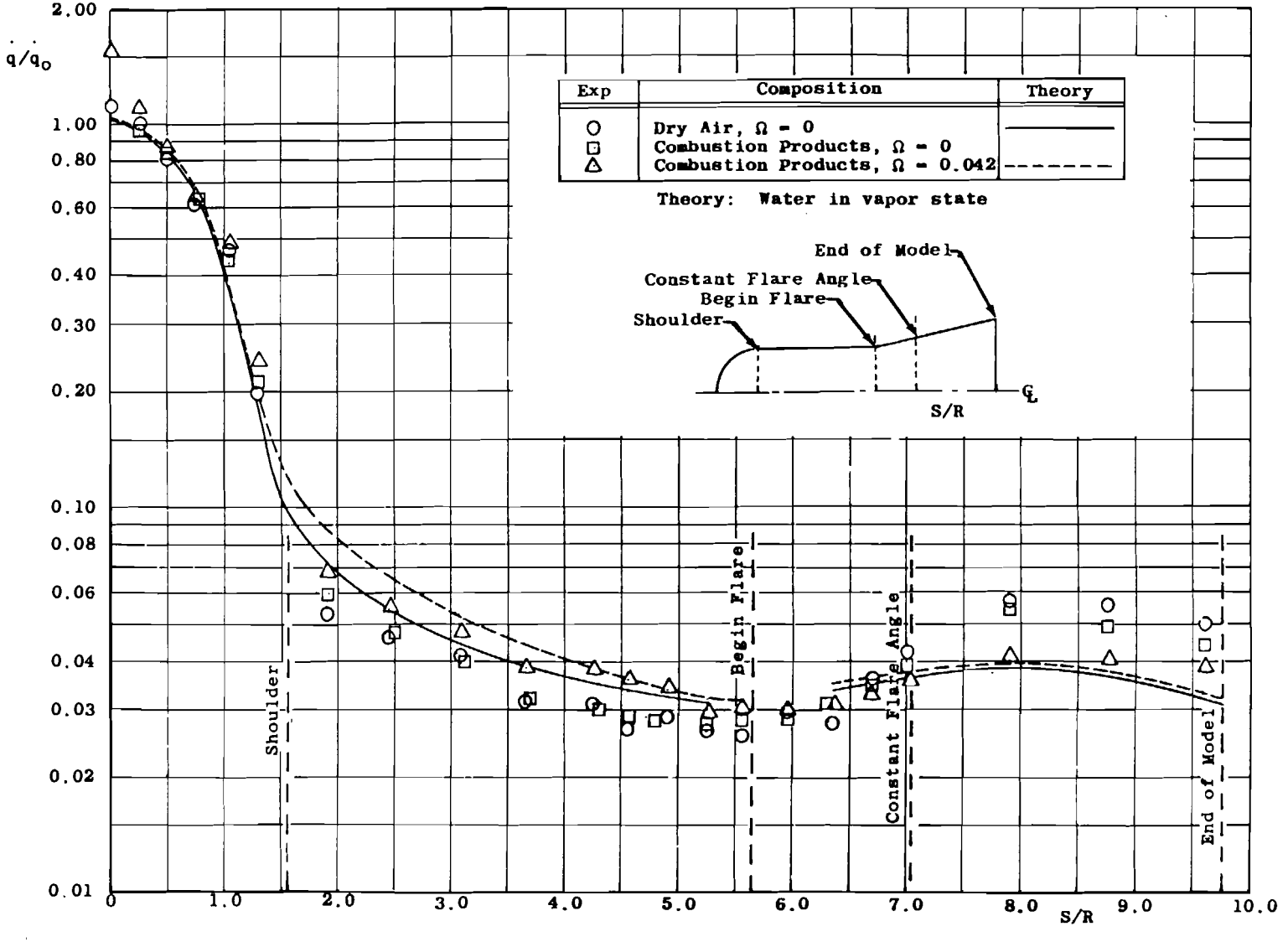

Fig. 12 Heat Transfer Rate Distribution on the Flared Hemispherical Cylinder, $\alpha = 0$ deg

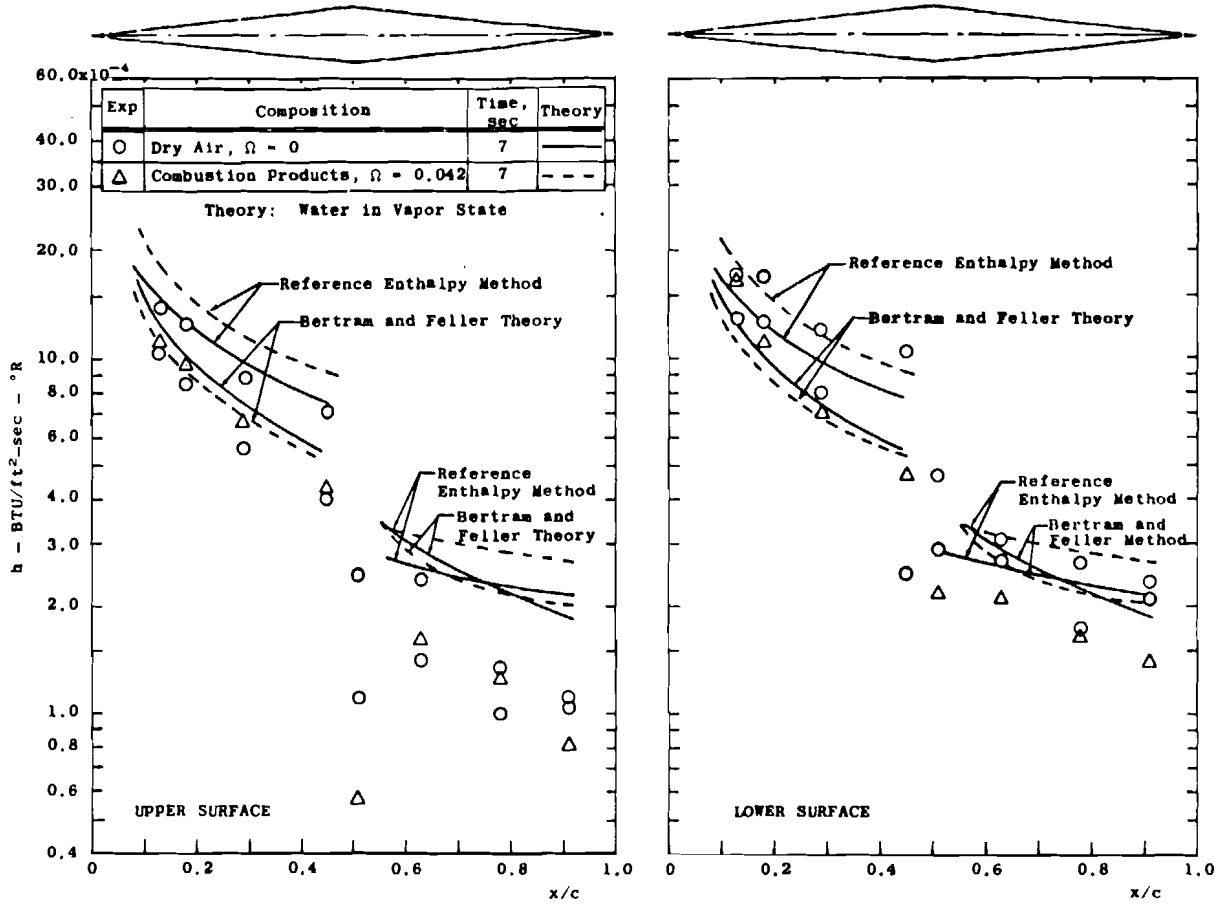

a. α = 0 deg

Fig. 13 Heat Transfer Coefficient Distribution on Blunted 6-deg Half-Angle Double Wedge

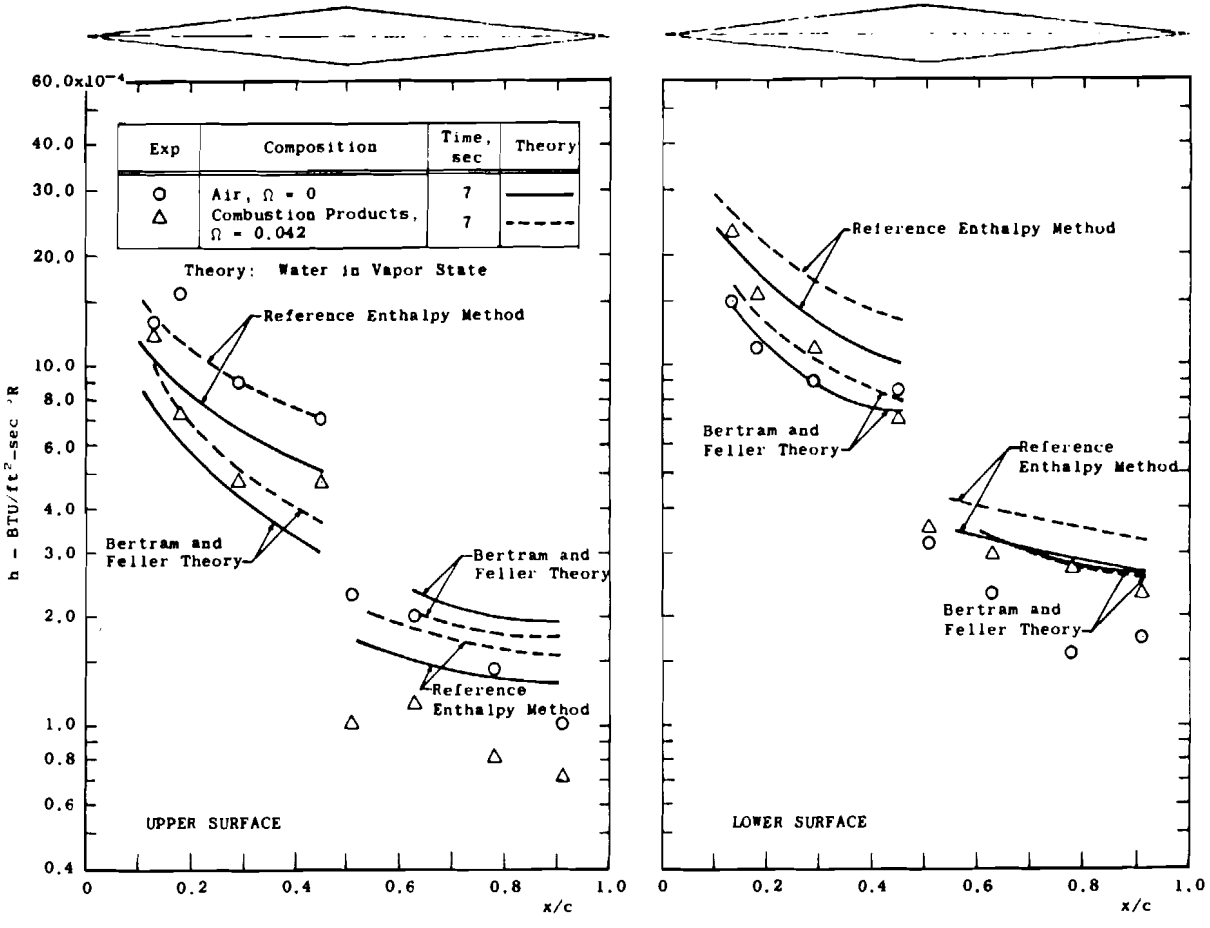

b. $\alpha = 5$ deg

Fig. 13 Continued

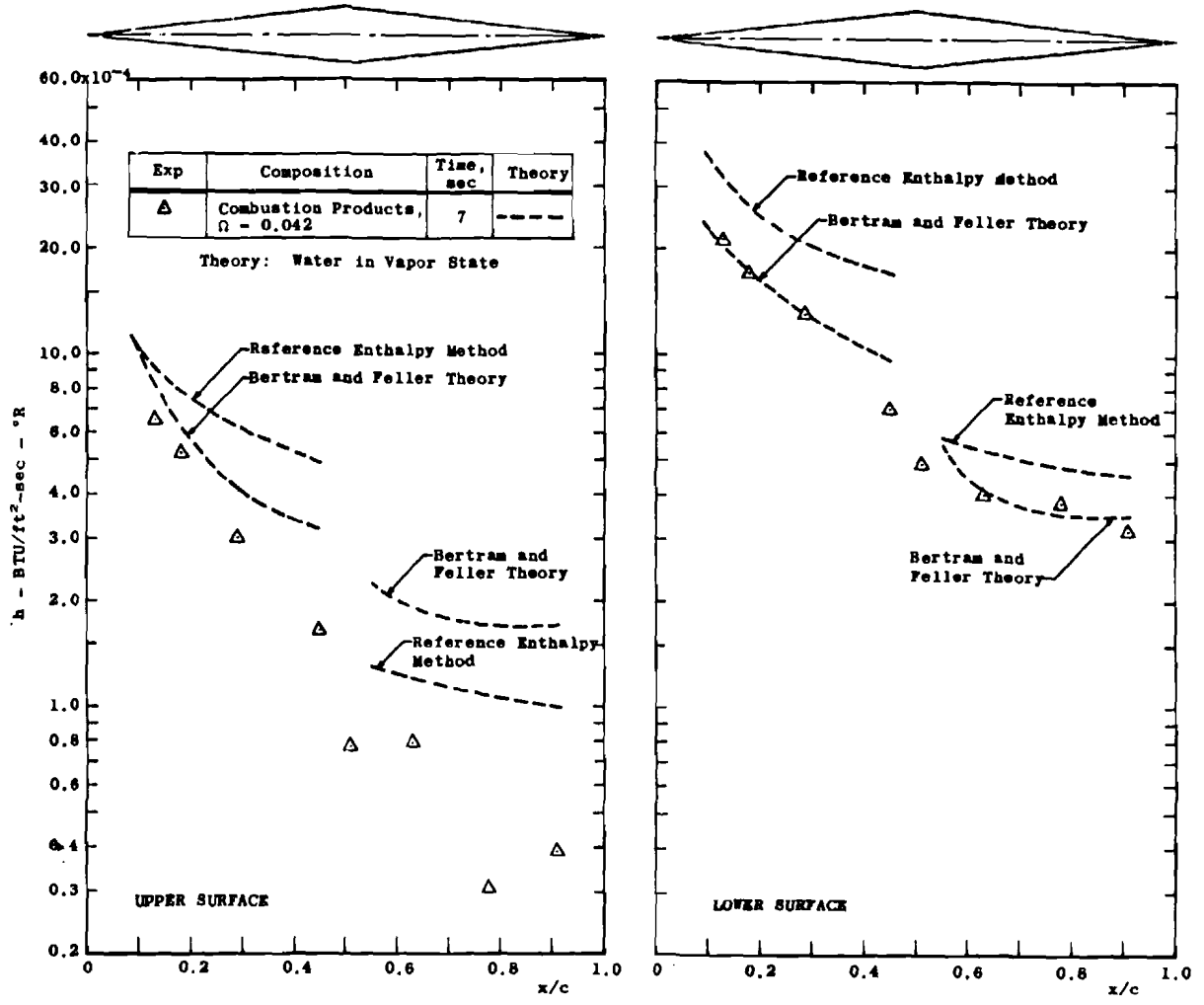

c. α = 10 deg

Fig. 13 Continued

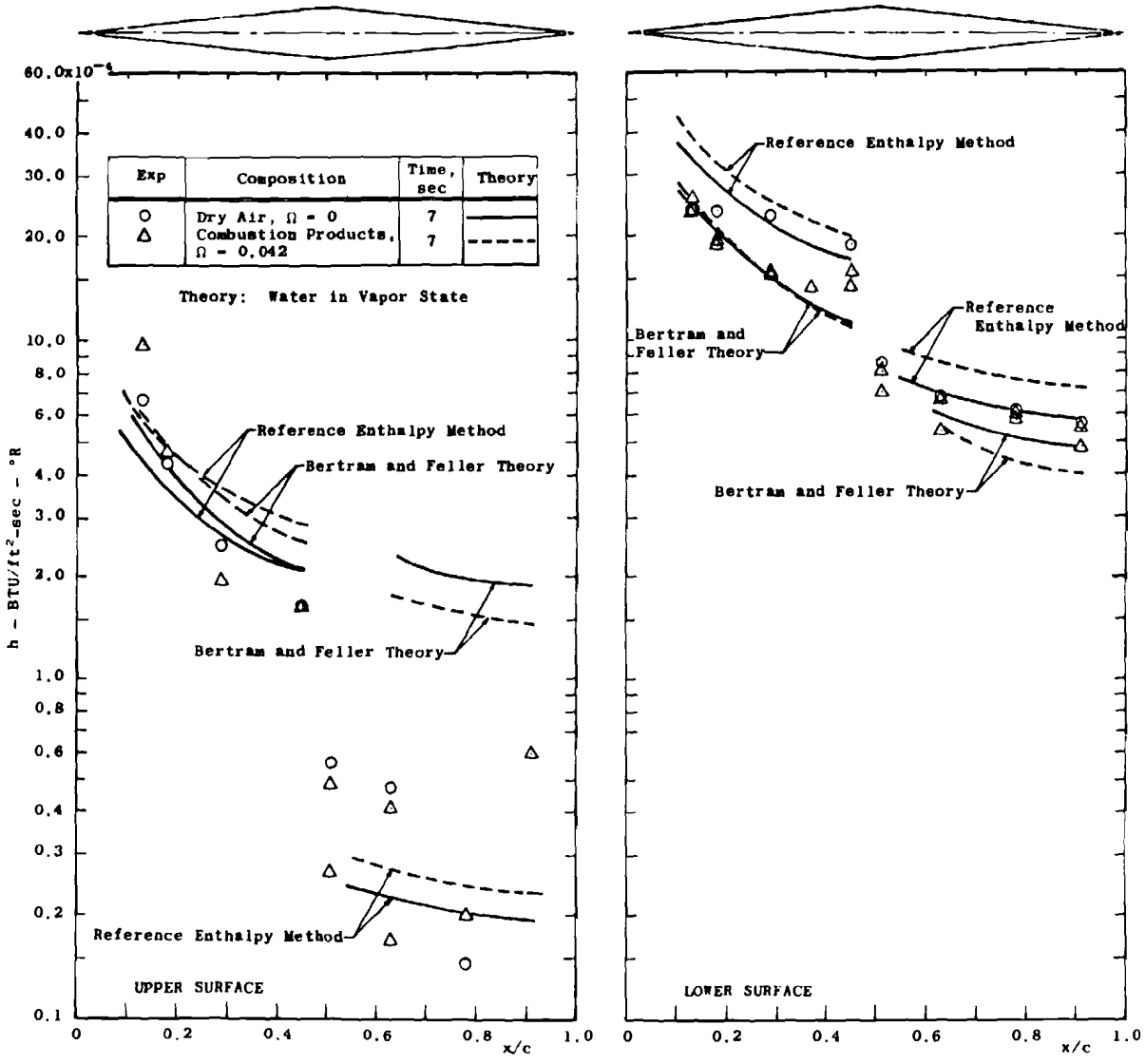

d. α = 15 deg

Fig. 13 Concluded

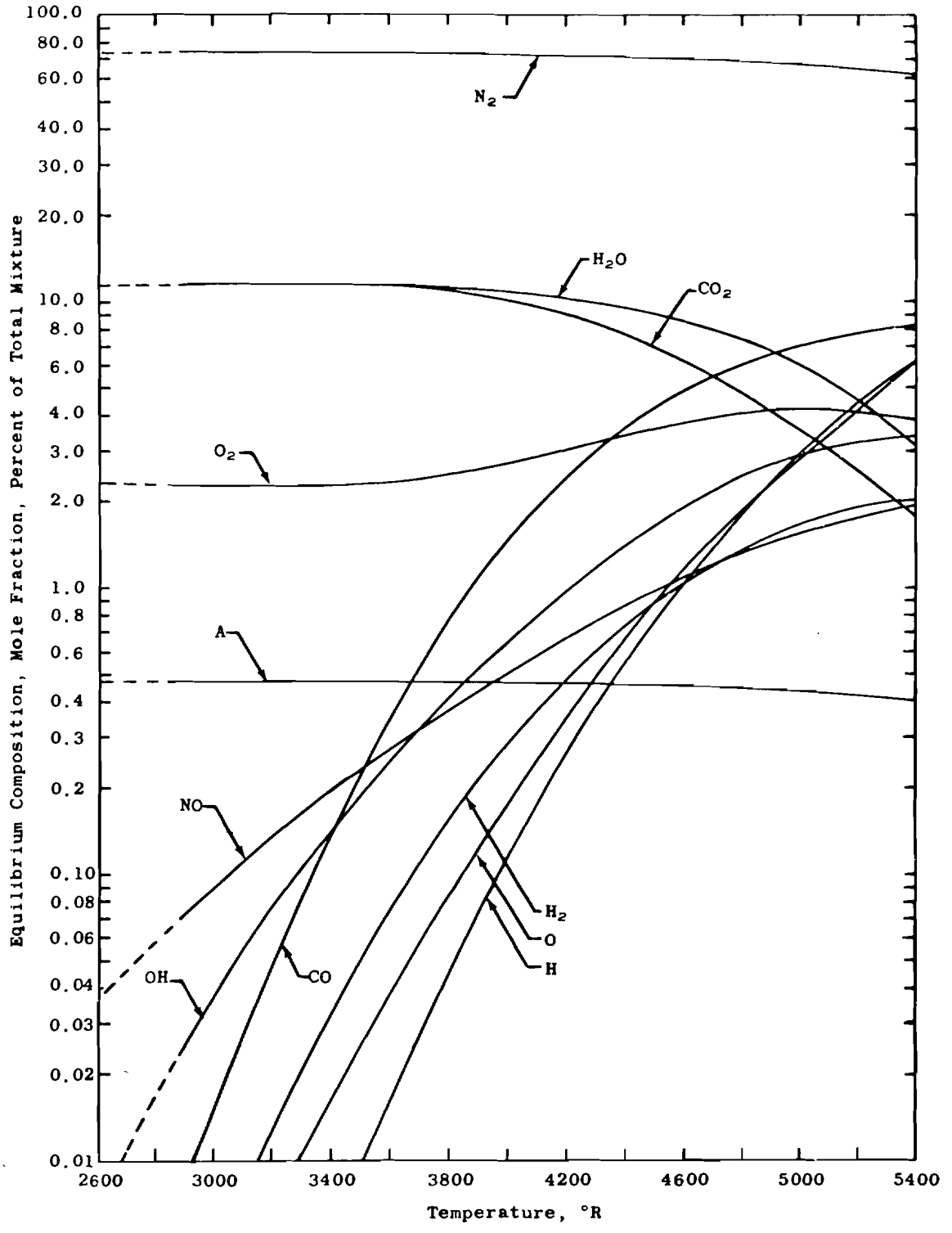

a. Combustion Gas, C_2H_4 and Air at f/a = 0.06, $\rho/\rho_o = 10^{-2}$

Fig. 14 Equilibrium Composition of Air and Combustion Gases

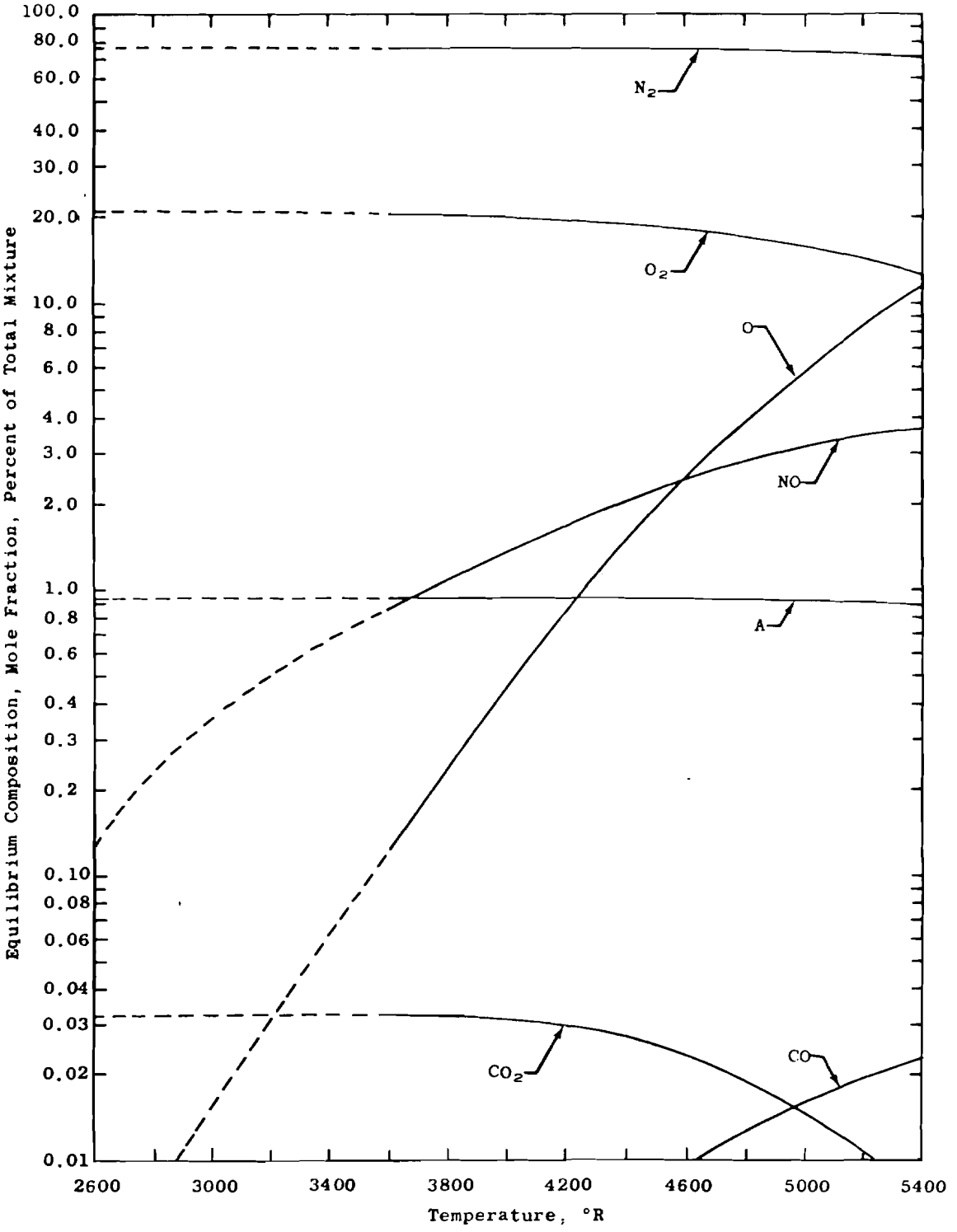

b. Air, $\rho/\rho_o = 10^{-2}$

Fig. 14 Concluded